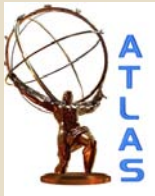
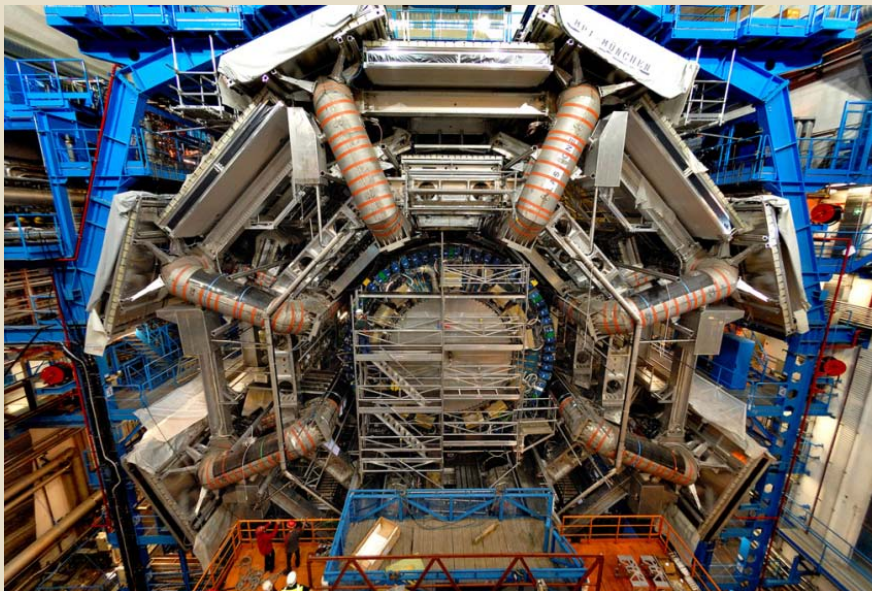


ATLAS Higgs searches in WW and ZZ channels

1

**LYDIA ICONOMIDOU-FAYARD (LAL-ORSAY)
ON BEHALF OF THE ATLAS COLLABORATION**



The ATLAS Detector

2

Multi-purpose detector at LHC
Details in JINST 3 (2008) S08003

→ Inner tracking system with silicon pixels , silicon microstrips and transition radiation detectors, immersed in a 2T field made by a solenoid SC magnet.

→ Liquid Argon EM Calorimetry, projectively segmented in 3 layers and hermetic in φ .

→ Hadronic Calorimetry
(Scintillating tiles or Larg)

→ Muon spectrometer operating in a large SC toroid magnet system.

The ATLAS Detector

3

Multi-purpose detector at LHC
Details in JINST 3 (2008) S08003

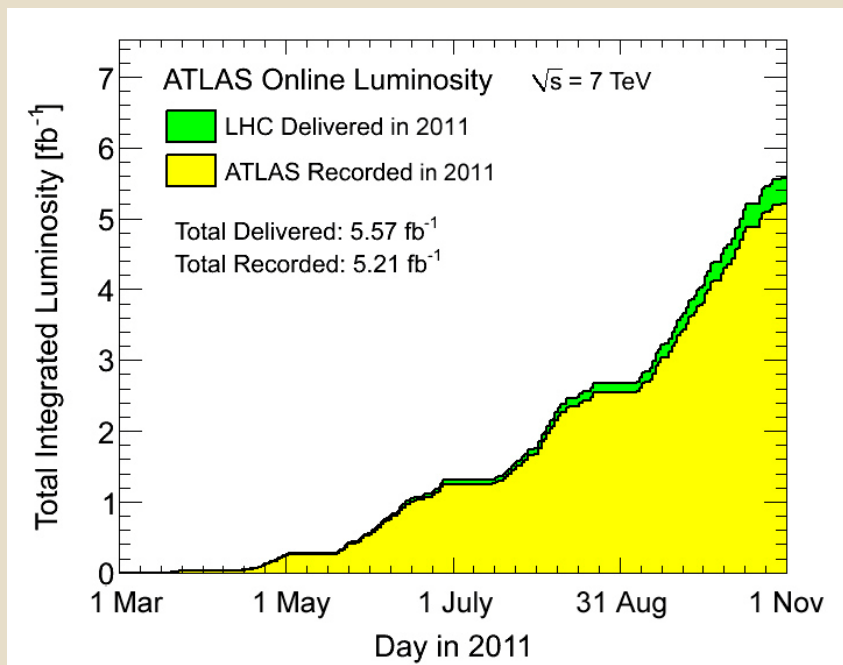
→ Inner tracking system with silicon pixels , silicon microstrips and transition radiation detectors, immersed in a 2T field made by a solenoid SC magnet.

→ Liquid Argon EM Calorimetry, projectively segmented in 3 layers and hermetic in φ

→ Hadronic Calorimetry (Scintillating tiles or Larg)

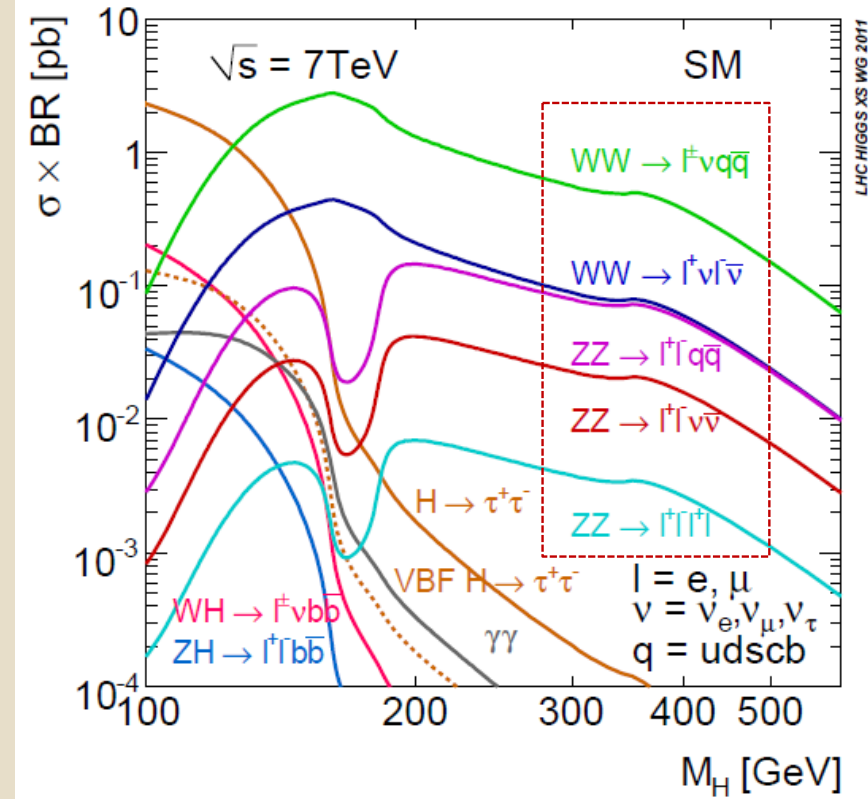
→ Muon spectrometer operating in a large SC toroid magnet system.

→ ATLAS collected 5.2 fb^{-1} by the end of the proton-proton run at $\sqrt{s}=7\text{TeV}$.
→ Average efficiency over 2011 : ~93%



The Higgs decays through Diboson channels

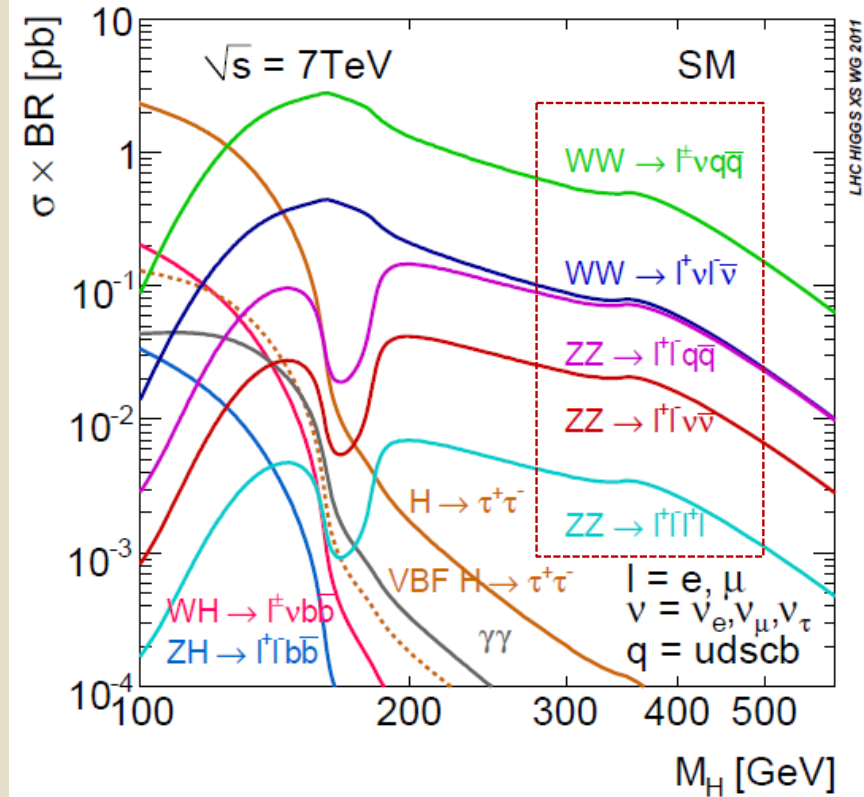
4



The Higgs decays through Diboson channels

5

→ Span a large M_H range

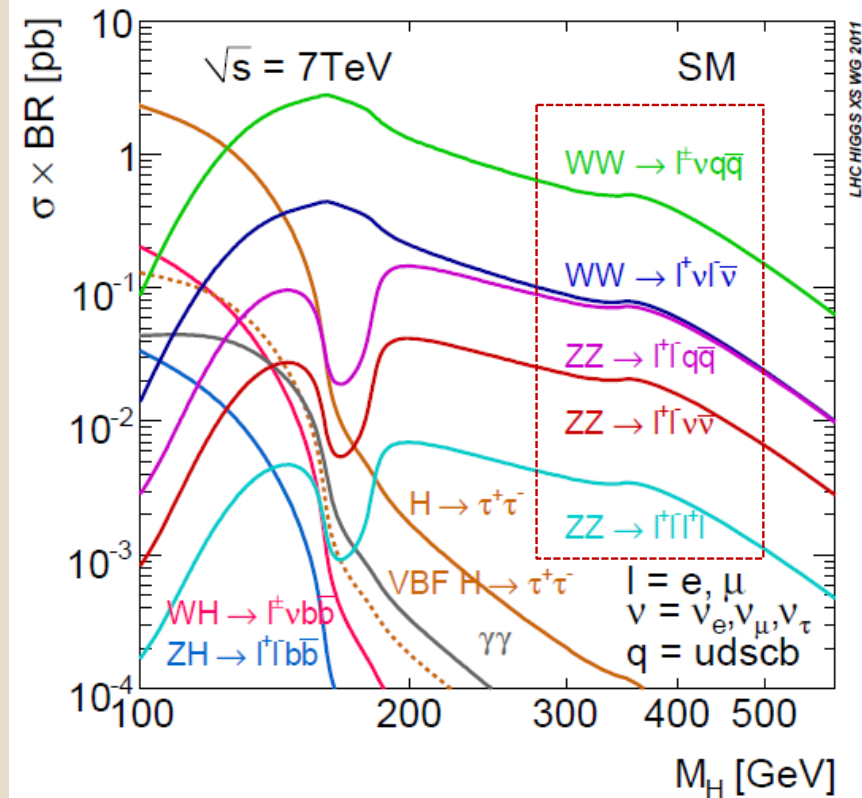


The Higgs decays through Diboson channels

6

→ Span a large M_H range

→ WW are the most abundant channels for $M_H > \sim 135\text{GeV}$.
Not all final state particles are fully measured



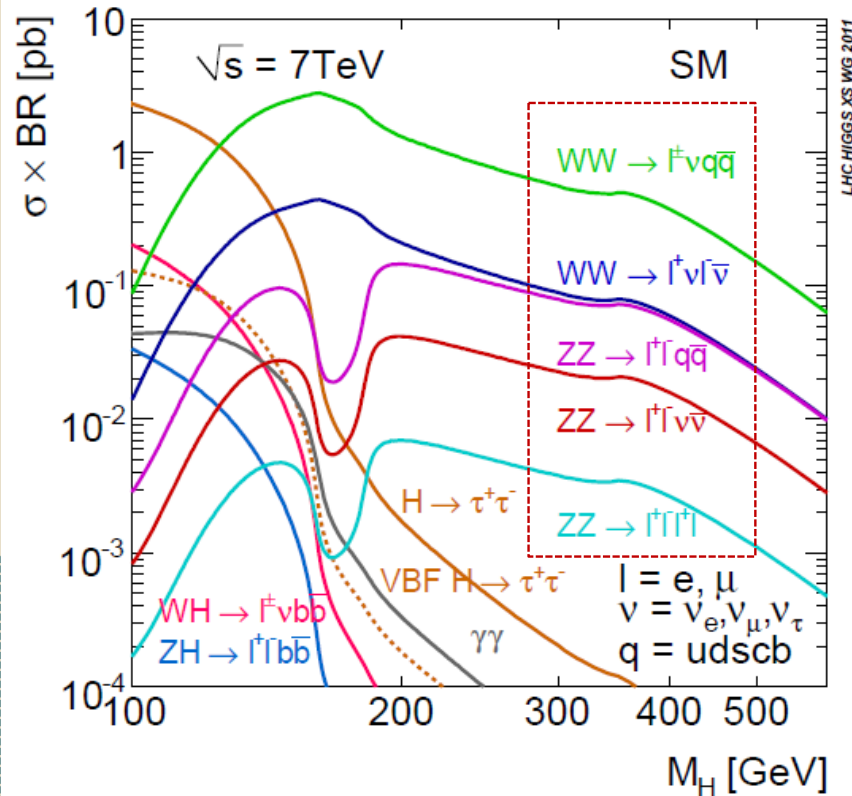
The Higgs decays through Diboson channels

7

→ Span a large M_H range

→ WW are the most abundant channels for $M_H > \sim 135\text{GeV}$.
Not all final state particles are fully measured

→ ZZ smaller rate but advantage from the full reconstruction of at least one on-shell Z.
Sharp peak for $ZZ \rightarrow 4l$.

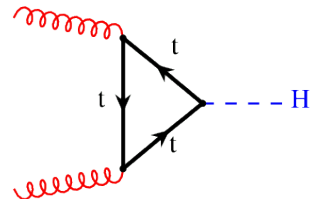


Signal and background yields

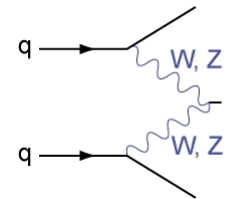
8

Signal and background yields

9



gg \rightarrow H : NNLO QCD
NNLL for soft gluon
NLO for EW

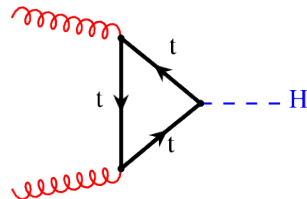


qq \rightarrow Hqq (VBF):
NNLO QCD
NLO for EW

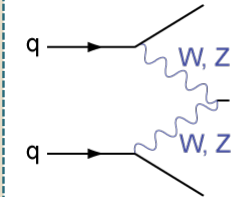
CROSS-SECTIONS

Signal and background yields

10



gg \rightarrow H : NNLO QCD
NNLL for soft gluon
NLO for EW



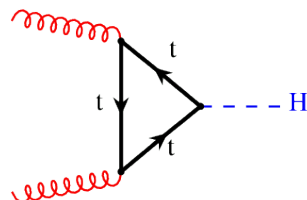
qq \rightarrow Hqq (VBF):
NNLO QCD
NLO for EW

CROSS-SECTIONS

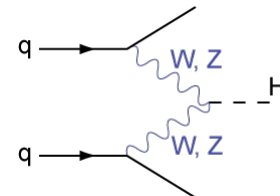
LHC Higgs Cross-Section Working Group arXiv:1101.0593 [hep-ph]

Signal and background yields

11



gg \rightarrow H : NNLO QCD
NNLL for soft gluon
NLO for EW



qq \rightarrow Hqq (VBF):
NNLO QCD
NLO for EW

LHC Higgs Cross-Section Working Group arXiv:1101.0593 [hep-ph]

CROSS-SECTIONS

PYTHIA
ALPGEN
HERWIG for parton showering and hadronization
MC@NLO
JIMMY for the underlying event
MCFM

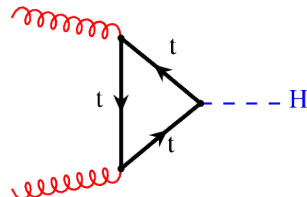
SIGNAL

POWHEG –Pythia
Reweight of the H PT spectrum
PhOTOS for FS QED radiative corrections
TAUOLA
MC@NLO
H \rightarrow ZZ \rightarrow 4l PROPHECY4F for BR

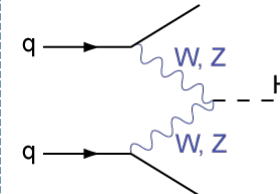
BACKGROUNDS

Signal and background yields

12



$gg \rightarrow H$: NNLO QCD
NNLL for soft gluon
NLO for EW



$qq \rightarrow Hqq$ (VBF):
NNLO QCD
NLO for EW

LHC Higgs Cross-Section Working Group arXiv:1101.0593 [hep-ph]

SIGNAL

POWHEG –Pythia

Reweighting of the H PT spectrum

PhoTOS for FS QED radiative corrections

TAUOLA

MC@NLO

$H \rightarrow ZZ \rightarrow 4l$ PROPHECY4F for BR

BACKGROUNDS

PYTHIA

ALPGEN

HERWIG for parton showering and hadronization

MC@NLO

JIMMY for the underlying event

MCFM



Higgs \rightarrow WW $^{(*)}$

13

Two channels :

- $H \rightarrow WW^{(*)} \rightarrow \ell^+ \nu \ell^- \bar{\nu}$ with $\ell = \mu, e$ (in 110-300GeV)
(with 1.7 fb $^{-1}$ of data ATLAS-CONF-2011-134)

- $H \rightarrow WW^{(*)} \rightarrow l\nu jj$ with $l = e, \mu$ (in 240-600GeV)
(with 1.04fb $^{-1}$ of data arXiv:1109.3615v1 [hep-ex])

Higgs \rightarrow WW $^{(*)}$

14

Two channels :

- $H \rightarrow WW^{(*)} \rightarrow \ell^+ \nu \ell^- \bar{\nu}$ with $\ell = \mu, e$ (in 110-300GeV)
(with 1.7 fb^{-1} of data ATLAS-CONF-2011-134)
- $H \rightarrow WW^{(*)} \rightarrow l\nu jj$ with $l = e, \mu$ (in 240-600GeV)
(with 1.04 fb^{-1} of data arXiv:1109.3615v1 [hep-ex])

Common feature:
Isolated lepton(s) and
missing transverse momentum

$H \rightarrow W W^{(*)} \rightarrow l\nu jj$: analysis and results

15

- One single lepton $P_T > 30\text{GeV}$, well identified and isolated
- $E_T^{\text{miss}} > 30\text{ GeV}$
- 2 ($H+0$) or 3 ($H+1$) jets with one $71 < M(jj) < 91\text{ GeV}$

$H \rightarrow W W^{(*)} \rightarrow l\nu jj$: analysis and results

16

- One single lepton $P_T > 30\text{GeV}$, well identified and isolated
- $E_T\text{miss} > 30\text{ GeV}$
- 2 (H+0) or 3 (H+1) jets with one $71 < M(jj) < 91\text{ GeV}$
- Reconstruct $M(l\nu jj)$ from $P_T(l)$, $E_T\text{miss}$ and from the 2 jets, imposing $M(l\nu) = M_W$

$H \rightarrow W W^{(*)} \rightarrow l\nu jj$: analysis and results

17

- One single lepton $P_T > 30\text{GeV}$, well identified and isolated
- $E_T\text{miss} > 30\text{ GeV}$
- 2 ($H+0$) or 3 ($H+1$) jets with one $71 < M(jj) < 91\text{ GeV}$
- Reconstruct $M(l\nu jj)$ from $P_T(l)$, $E_T\text{miss}$ and from the 2 jets, imposing $M(l\nu) = M_W$

Backgrounds :

- $W + \text{Jets}$, $Z + \text{Jets}$ and Top modelled by MC.
- MultiJets assessed by data driven methods

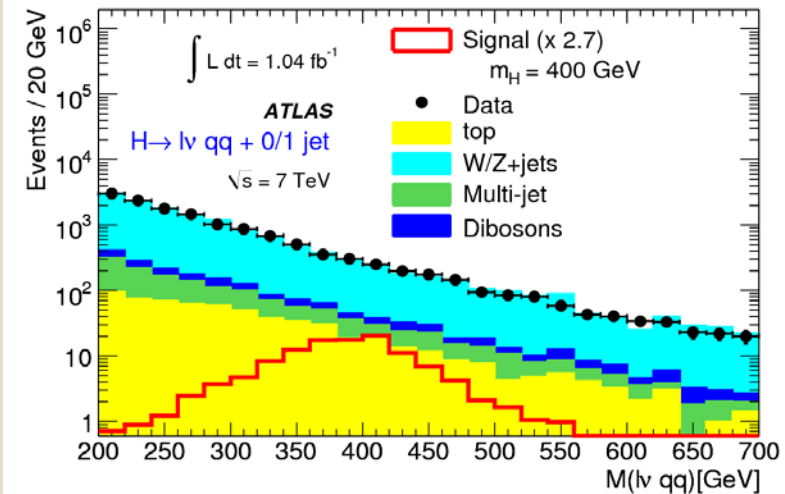
$H \rightarrow W W^{(*)} \rightarrow l\nu jj$: analysis and results

18

- One single lepton $P_T > 30\text{ GeV}$, well identified and isolated
- $\text{ETmiss} > 30\text{ GeV}$
- 2 ($H+0$) or 3 ($H+1$) jets with one $71 < M(jj) < 91\text{ GeV}$
- Reconstruct $M(l\nu jj)$ from $P_T(l)$, ETmiss and from the 2 jets, imposing $M(l\nu) = M_W$

Backgrounds :

- $W + \text{Jets}$, $Z + \text{Jets}$ and Top modelled by MC.
- MultiJets assessed by data driven methods



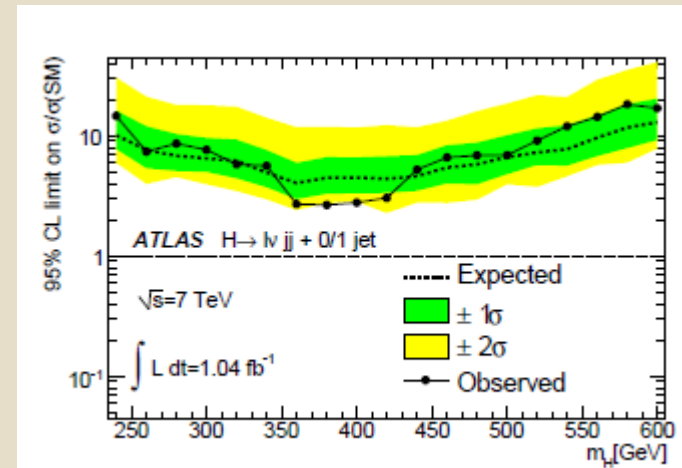
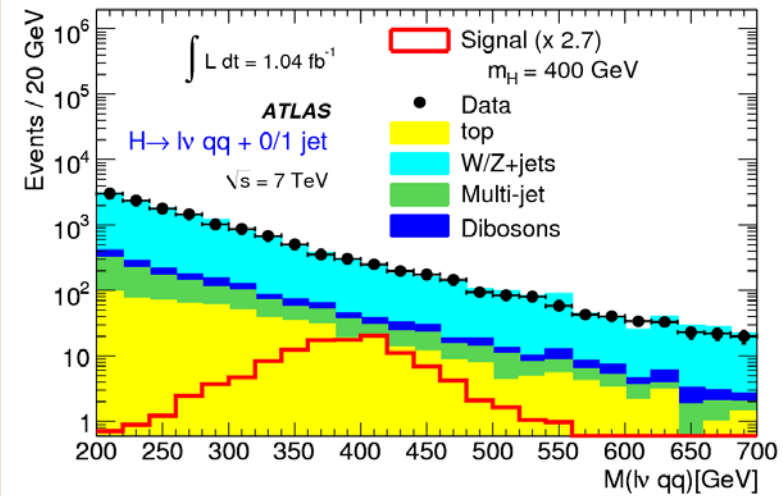
H \rightarrow WW (*) \rightarrow lν jj : analysis and results

19

- One single lepton $P_T > 30\text{ GeV}$, well identified and isolated
- $E_{T\text{miss}} > 30\text{ GeV}$
- 2 (H+0) or 3 (H+1) jets with one $71 < M(\text{jj}) < 91\text{ GeV}$
- Reconstruct $M(l\nu jj)$ from $P_T(l)$, $E_{T\text{miss}}$ and from the 2 jets, imposing $M(l\nu) = M_W$

Backgrounds :

- W+Jets, Z+Jets and Top modelled by MC.
- MultiJets assessed by data driven methods

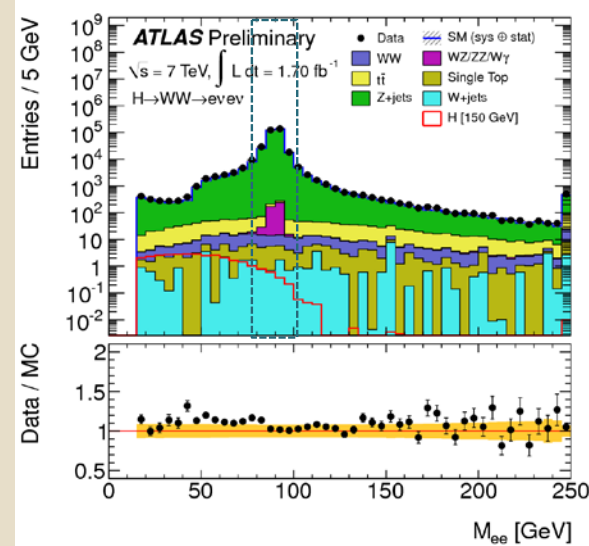


$H \rightarrow WW^* \rightarrow l^+ l^- : selection$

20

Require

- Opposite charge leptons
- Apply Y and Z veto in $m(l\bar{l})$
($m_{l\bar{l}} > 15 \text{ GeV}$, $|M_Z - M_{l\bar{l}}| > 15 \text{ GeV}$)



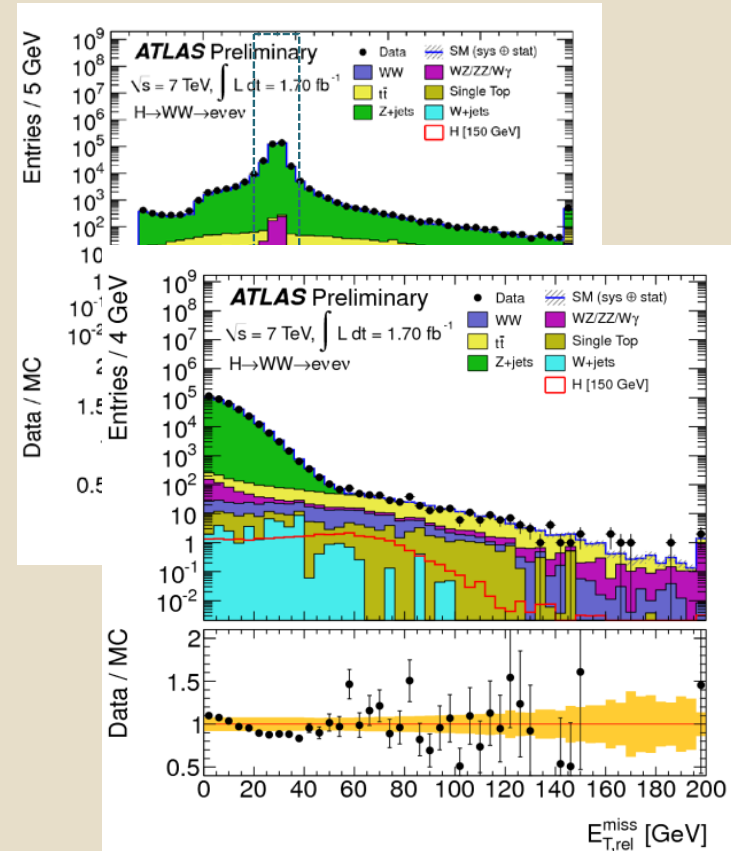
$H \rightarrow WW^* \rightarrow l^+ l^- : selection$

21

Require

- Opposite charge leptons
- Apply Y and Z veto in $m(l\bar{l})$
($m_{l\bar{l}} > 15 \text{ GeV}$, $|M_Z - M_{l\bar{l}}| > 15 \text{ GeV}$)

→ $E_T^{\text{miss}} > 40(25) \text{ GeV}$ for
same / different flavor



$H \rightarrow WW^* \rightarrow l^+ l^- : selection$

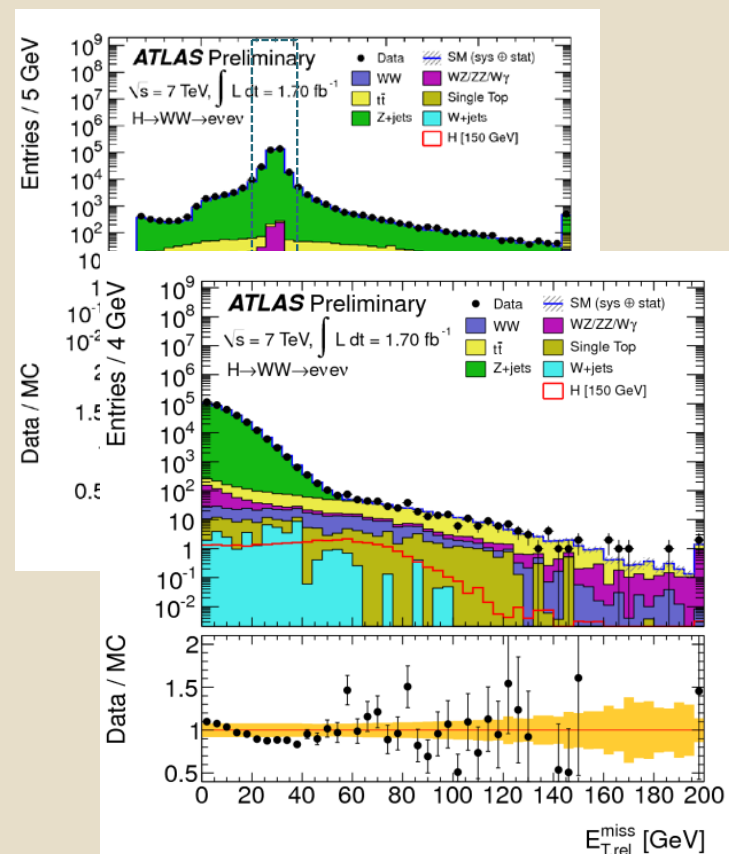
22

Require

- Opposite charge leptons
- Apply Y and Z veto in $m(l\bar{l})$
($m_{l\bar{l}} > 15 \text{ GeV}$, $|M_Z - M_{l\bar{l}}| > 15 \text{ GeV}$)

→ $E_T^{\text{miss}} > 40(25) \text{ GeV}$ for
same / different flavor

Major Backgrounds:
top, W+j, Z+j, SM WW
Estimated from data driven
methods



$H \rightarrow WW^* \rightarrow l^+ l^- : selection$

23

Require

- Opposite charge leptons
- Apply Y and Z veto in $m(l\bar{l})$
($m_{l\bar{l}} > 15\text{ GeV}$, $|M_Z - M_{l\bar{l}}| > 15\text{ GeV}$)

→ $E_T\text{miss} > 40(25)\text{ GeV}$ for
same /different flavor

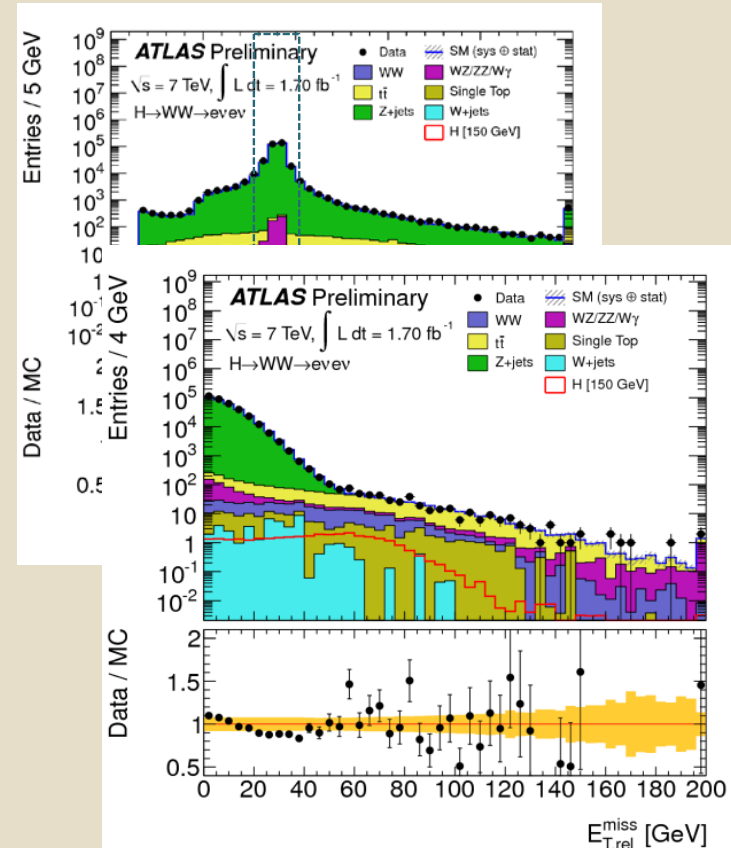
Different cuts for $H+0$, $H+1\text{jet}$:

- 0-Jet : $P_T(l\bar{l}) > 30\text{ GeV}$
- 1-Jet : Reject b-jet, $P_T > 25\text{ GeV}$,
 $(P_T(l1) + P_T(l2) + P_T(\text{jet}) + E_T\text{miss}) < 30\text{ GeV}$,
 $Z \rightarrow \tau\tau$ veto

Major Backgrounds: top, $W+j$,

$Z+j$, SM WW

Estimated from data driven
methods



$H \rightarrow WW^* \rightarrow l^+ l^- : selection$

24

Require

- Opposite charge leptons
- Apply Y and Z veto in $m(l\bar{l})$
($m_{l\bar{l}} > 15\text{ GeV}$, $|M_Z - M_{l\bar{l}}| > 15\text{ GeV}$)

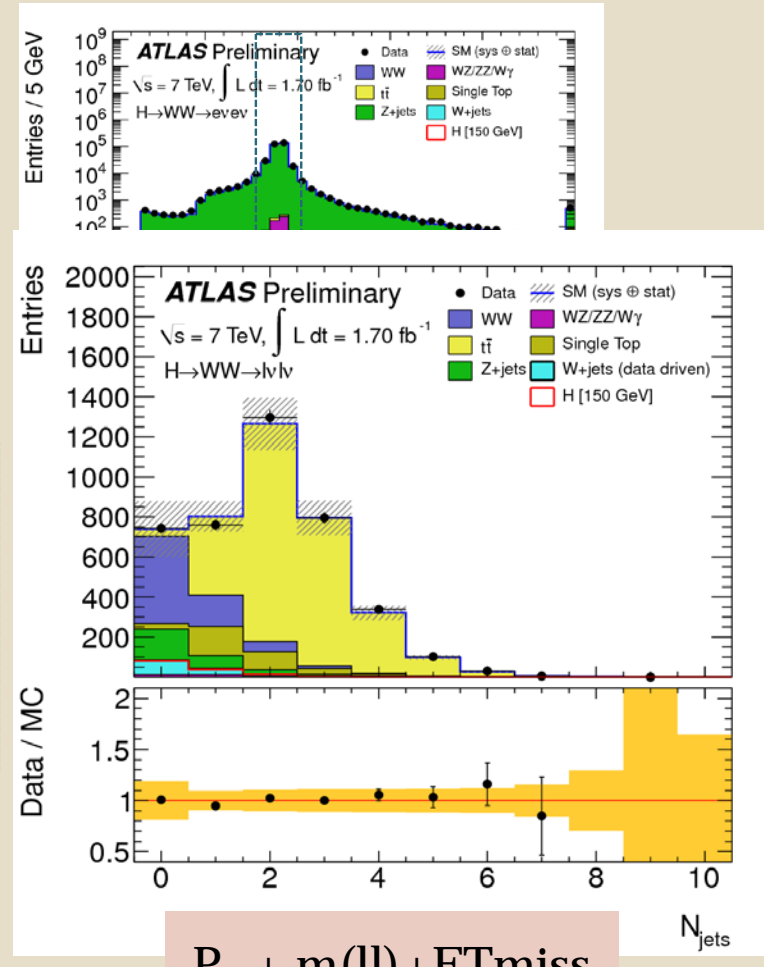
→ $E_T\text{miss} > 40(25)\text{ GeV}$ for
same /different flavor

Different cuts for $H+0$, $H+1\text{jet}$:

- 0-Jet : $P_T(l\bar{l}) > 30\text{ GeV}$
- 1-Jet : Reject b-jet, $P_T > 25\text{ GeV}$,
 $(P_T(l1) + P_T(l2) + P_T(\text{jet}) + E_T\text{miss}) < 30\text{ GeV}$,
 $Z \rightarrow \tau\tau$ veto

Major Backgrounds: top, $W+j$,
 $Z+j$, SM WW

Estimated from data driven
methods



$H \rightarrow WW^{(*)} \rightarrow l^+ \nu l^- \nu$: selection (2)

25

Other cuts M_H dependent

Cut on the transverse mass

$$m_T = \sqrt{(E_T^{\ell\ell} + E_T^{\text{miss}})^2 - (\mathbf{p}_T^{\ell\ell} + \mathbf{p}_T^{\text{miss}})^2}$$

$0.75 * M_H < M_T < M_H$ for $M_H < 220 \text{ GeV}$

$0.6 * M_H < M_T < M_H$ otherwise

Rejection of top and WW backgrounds:

Cuts on $m(l\bar{l})$ and $\Delta\Phi(l\bar{l})$

$m(l\bar{l}) < 50$ (65) for $M_H < 170$ (220) GeV

$50 < m(l\bar{l}) < 180$ for $M_H > 220$ GeV

$\Delta\Phi(l\bar{l}) < 1.3$ (1.8) for $M_H < 170$ (220) GeV

$H \rightarrow WW^* \rightarrow l^+ l^- \nu \bar{\nu}$: selection (2)

26

Other cuts M_H dependent

Cut on the transverse mass

$$m_T = \sqrt{(E_T^{\ell\ell} + E_T^{\text{miss}})^2 - (\mathbf{p}_T^{\ell\ell} + \mathbf{p}_T^{\text{miss}})^2}$$

$0.75 * M_H < M_T < M_H$ for $M_H < 220 \text{ GeV}$
 $0.6 * M_H < M_T < M_H$ otherwise

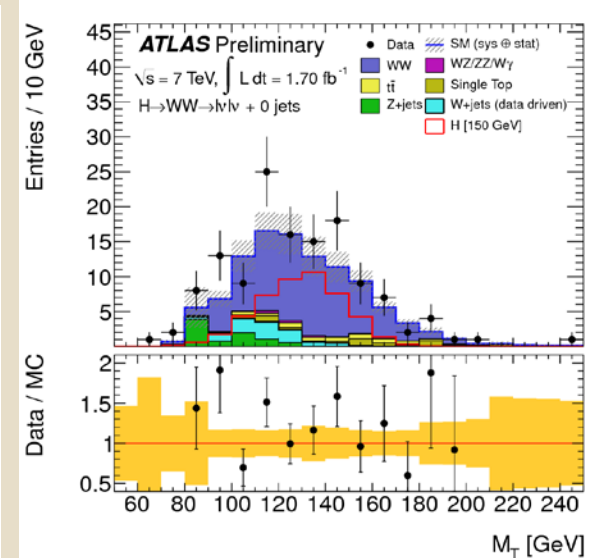
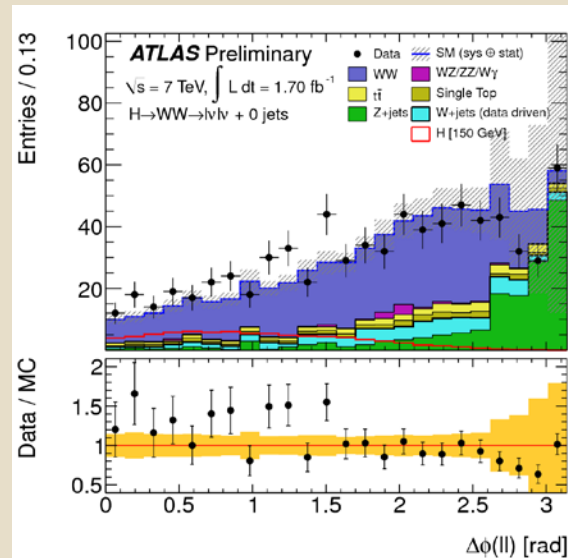
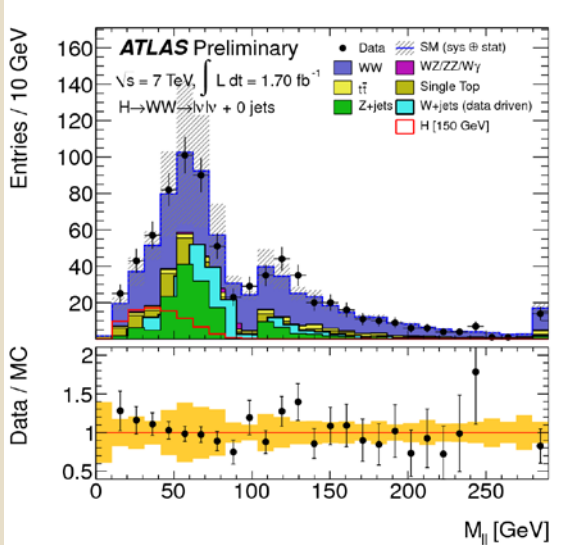
Rejection of top and WW backgrounds:

Cuts on $m(l\bar{l})$ and $\Delta\Phi(l\bar{l})$

$m(l\bar{l}) < 50$ (65) for $M_H < 170$ (220) GeV

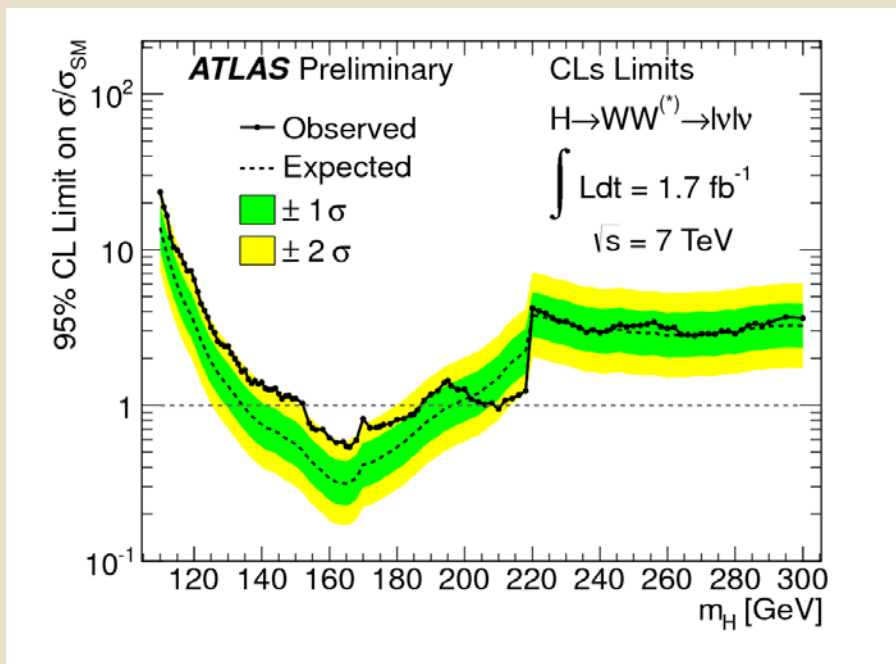
$50 < m(l\bar{l}) < 180$ for $M_H > 220$ GeV

$\Delta\Phi(l\bar{l}) < 1.3$ (1.8) for $M_H < 170$ (220) GeV



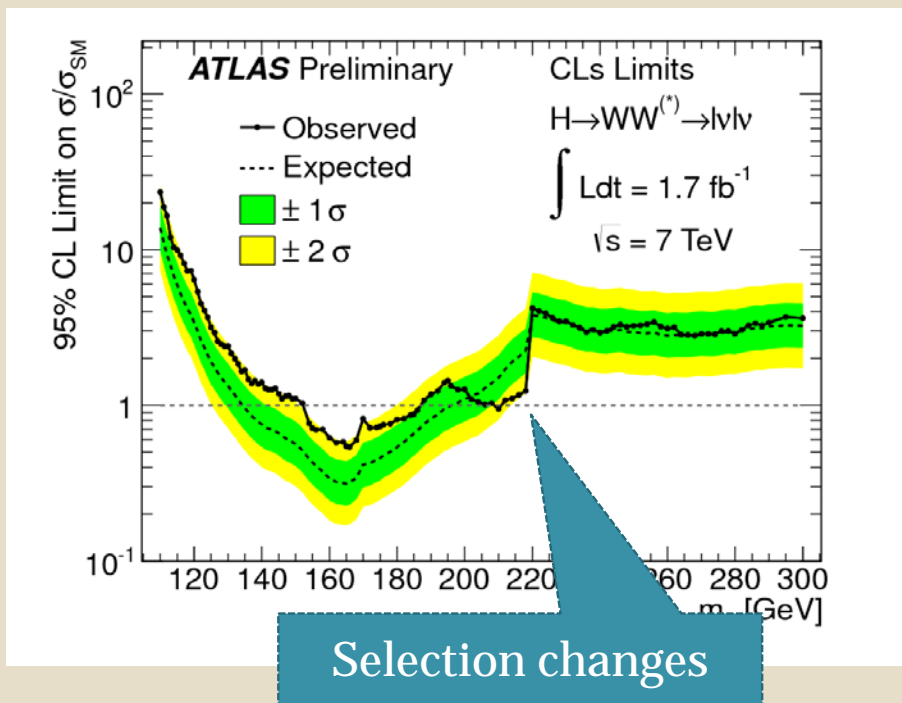
$H \rightarrow WW^{(*)} \rightarrow l^+ l^- \nu \bar{\nu}$: Results

27



$H \rightarrow WW^{(*)} \rightarrow l^+ l^- \nu \bar{\nu}$: Results

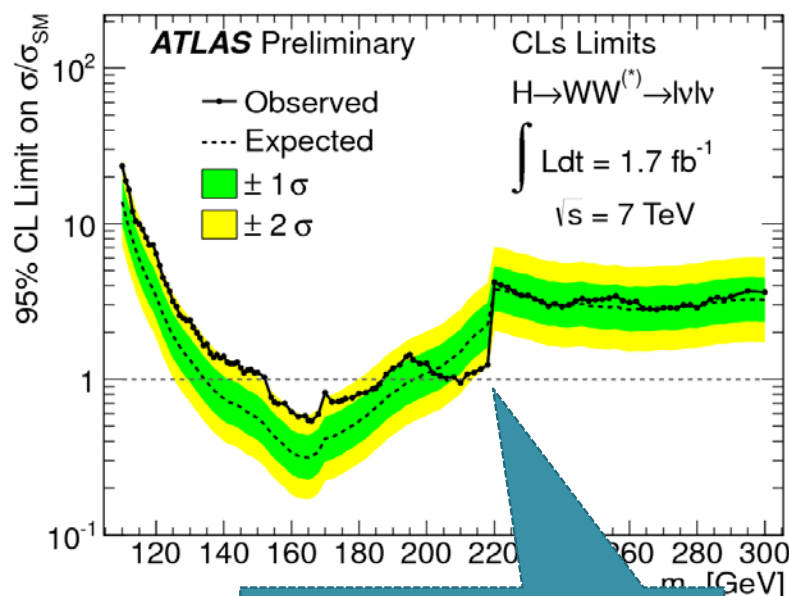
28



$H \rightarrow WW^{(*)} \rightarrow l^+ l^- \nu \bar{\nu}$: Results

29

Largest deviation from expectation : $\sim 2\sigma$



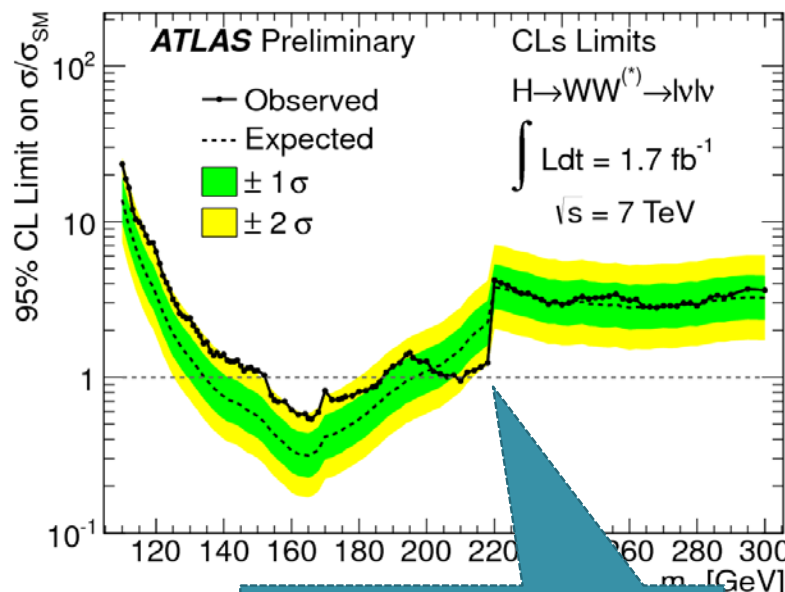
Excluded : $154 \text{ GeV} < M_H < 186 \text{ GeV}$

$H \rightarrow WW^{(*)} \rightarrow l^+ l^- \nu \bar{\nu}$: Results

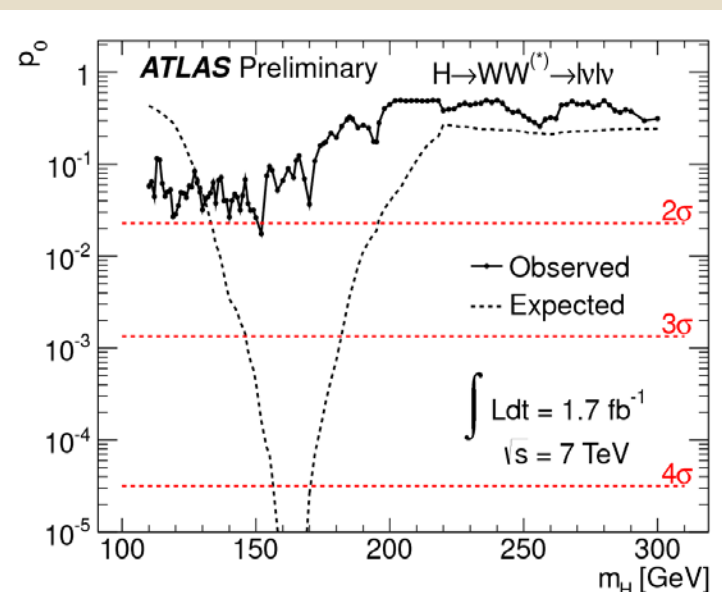
30

Largest deviation from expectation : $\sim 2\sigma$

p_0 value = probability for the background to fluctuate



Selection changes



Excluded : $154 \text{ GeV} < M_H < 186 \text{ GeV}$

Higgs \rightarrow ZZ $(*)$

31

Three channels :

- H \rightarrow ZZ $\rightarrow l^+l^- \nu\nu$ with l=μ, e (200-600 GeV)
(with 2.05fb $^{-1}$ of data NEW ATLAS-CONF-2011-148)
- H \rightarrow ZZ $\rightarrow l^+l^- qq$ with l=μ, e (200-600 GeV)
(with 2.05fb $^{-1}$ of data NEW ATLAS-CONF-2011-150)
- H \rightarrow ZZ $(*)$ $\rightarrow 4l$ with l=μ, e (120-600 GeV)
(with 2.1 fb $^{-1}$ LP result Phys. Lett. B 705 (2011) 435-451)

Higgs \rightarrow ZZ $(*)$

32

Three channels :

- H \rightarrow ZZ $\rightarrow l^+l^- vv$ with l= μ, e (200-600 GeV)
(with 2.05fb $^{-1}$ of data **NEW ATLAS-CONF-2011-148**)
- H \rightarrow ZZ $\rightarrow l^+l^- qq$ with l= μ, e (200-600 GeV)
(with 2.05fb $^{-1}$ of data **NEW ATLAS-CONF-2011-150**)
- H \rightarrow ZZ $(*) \rightarrow 4l$ with l= μ, e (120-600 GeV)
(with 2.1 fb $^{-1}$ LP result **Phys. Lett. B 705 (2011) 435-451**)

Common feature:
Isolated leptons and
at least one on-shell Z

H \rightarrow ZZ \rightarrow l⁺l⁻q \bar{q} (l=e or μ) selection

33

→ ZZ- \rightarrow llqq , both Zs on shell

Two leptons with $P_T > 20\text{ GeV}$, well identified , with isolated tracks and $M_{ll} \in [M_Z \pm 15] \text{ GeV}$

→ Z- \rightarrow qq: jets reconstructed using anti-Kt algorithm with $P_T > 25 \text{ GeV}$ and $M_{jj} \in [70,105]\text{GeV}$
→ E_{Tmiss}<50GeV

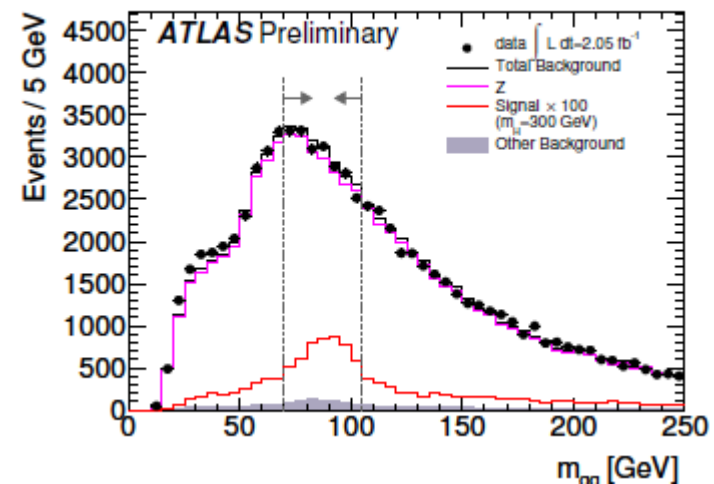
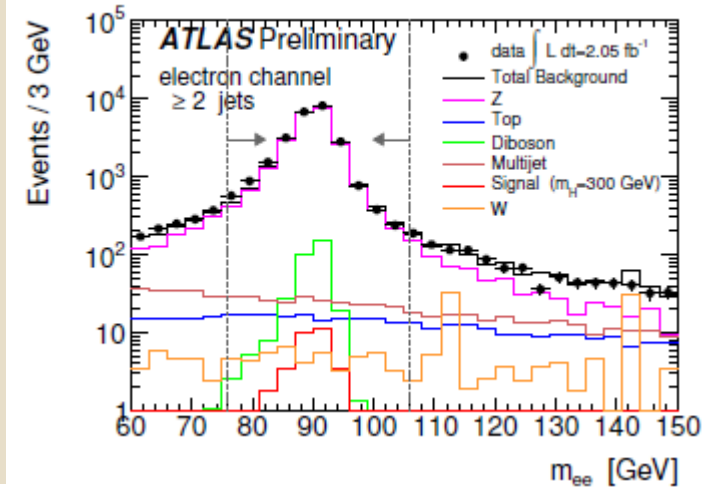
H \rightarrow ZZ \rightarrow l $^+$ l $^-$ q \bar{q} (l=e or μ) selection

34

→ ZZ- \rightarrow llqq , both Zs on shell

Two leptons with $P_T > 20\text{ GeV}$, well identified , with isolated tracks and $M_{ll} \in [M_Z \pm 15] \text{ GeV}$.

→ Z- \rightarrow qq: jets reconstructed using anti-Kt algorithm with $P_T > 25 \text{ GeV}$ and $M_{jj} \in [70,105]\text{GeV}$
→ E τ miss $< 50\text{GeV}$



$H \rightarrow ZZ \rightarrow l^+l^-q\bar{q}$ ($l=e$ or μ) selection

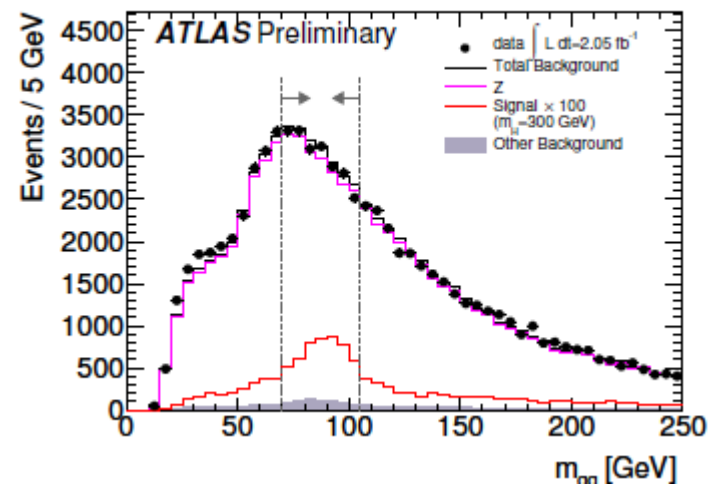
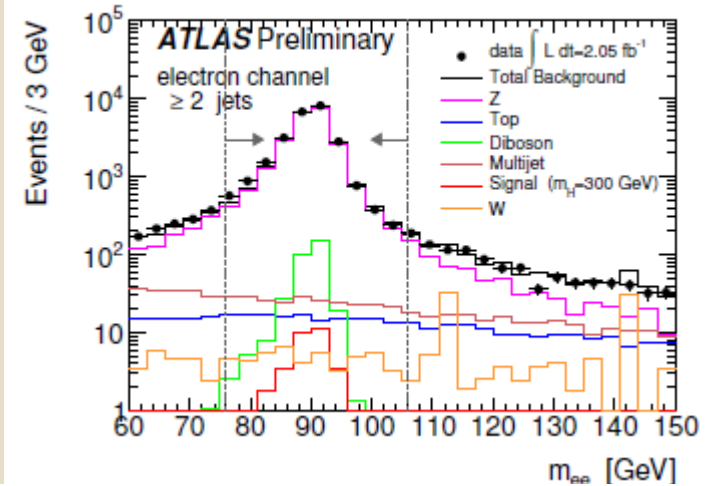
35

→ ZZ- $\rightarrow llqq$, both Zs on shell

Two leptons with $P_T > 20$ GeV, well identified, with isolated tracks and $M_{ll} \in [M_Z \pm 15]$ GeV

→ Z- $\rightarrow qq$: jets reconstructed using anti-Kt algorithm with $P_T > 25$ GeV and $M_{jj} \in [70, 105]$ GeV
→ $E_{T\text{miss}} < 50$ GeV

→ 20% of signal contain 2 b-jets.
Divide sample into Z+2 b-tagged jets and into Z+<2 tagged jets
→ tagging: 70% efficiency for a light jet rejection of 100



$H \rightarrow ZZ \rightarrow l^+l^-q\bar{q}$ ($l=e$ or μ) background

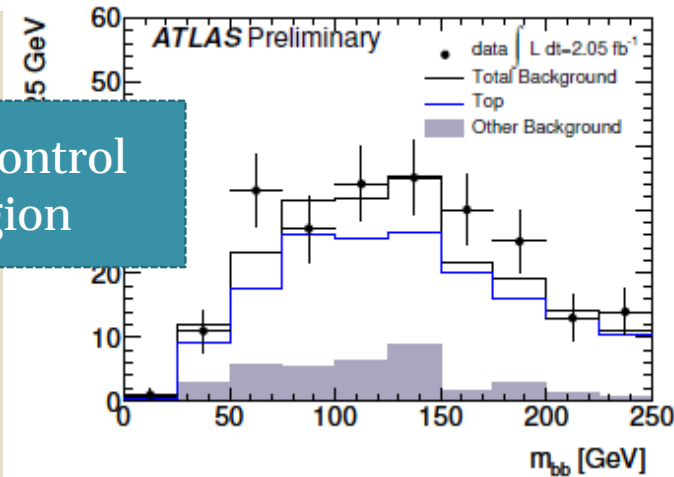
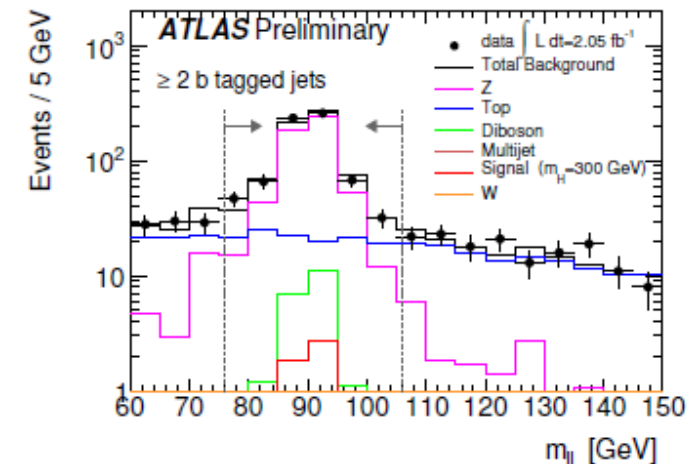
36

- Main backgrounds : $Z + \text{jets}$ and $t\bar{t}$
- Assessed with data-driven studies using M_{jj} or M_{ll} sidebands respectively

$H \rightarrow ZZ \rightarrow l^+l^-q\bar{q}$ ($l=e$ or μ) background

37

- Main backgrounds : $Z + \text{jets}$ and $t\bar{t}$
- Assessed with data-driven studies using M_{jj} or M_{ll} sidebands respectively

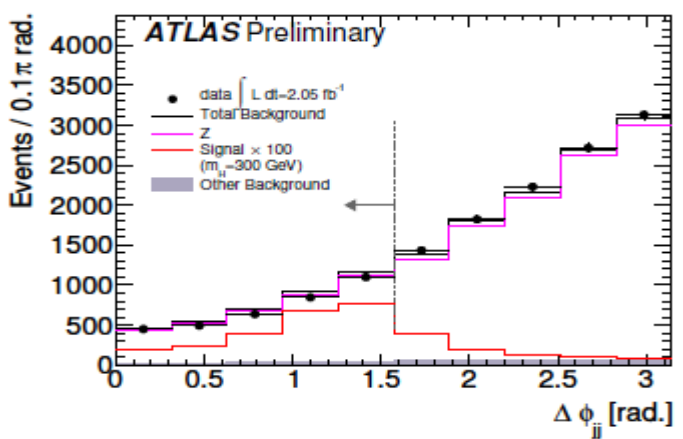


$H \rightarrow ZZ \rightarrow l^+l^-q\bar{q}$ ($l=e$ or μ) background

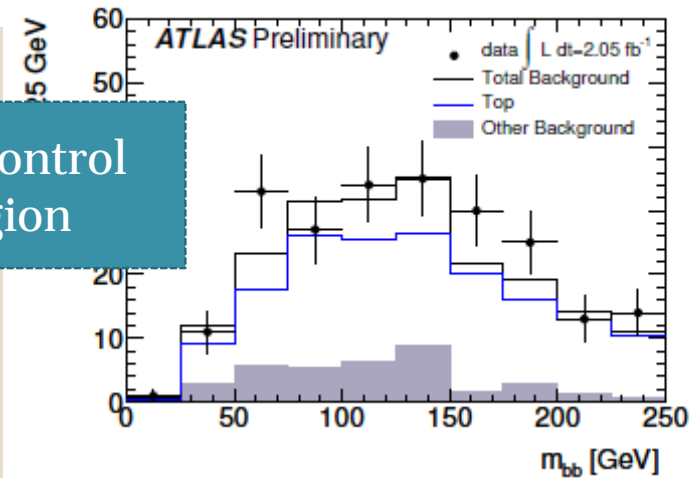
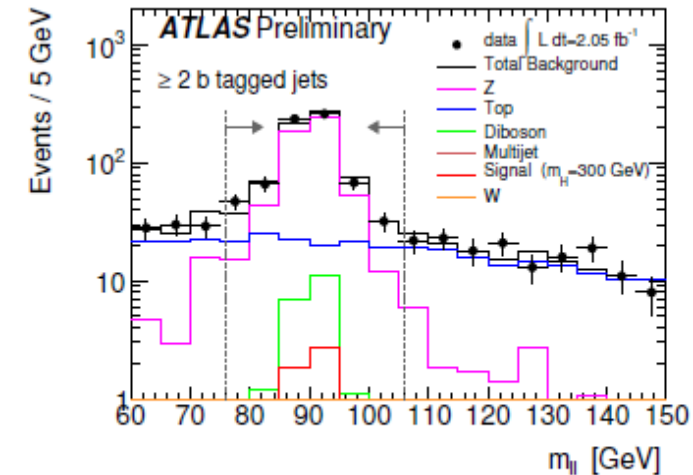
38

- Main backgrounds : $Z + \text{jets}$ and $t\bar{t}$
- Assessed with data-driven studies using M_{jj} or M_{ll} sidebands respectively

→ For $M_H > 300 \text{ GeV}$, angular kinematical cuts allow better rejection against $Z + \text{jets}$
 $\Delta\Phi(jj) < 90^\circ$, $\Delta\Phi(ll) < 90^\circ$, $P_T > 45 \text{ GeV}$



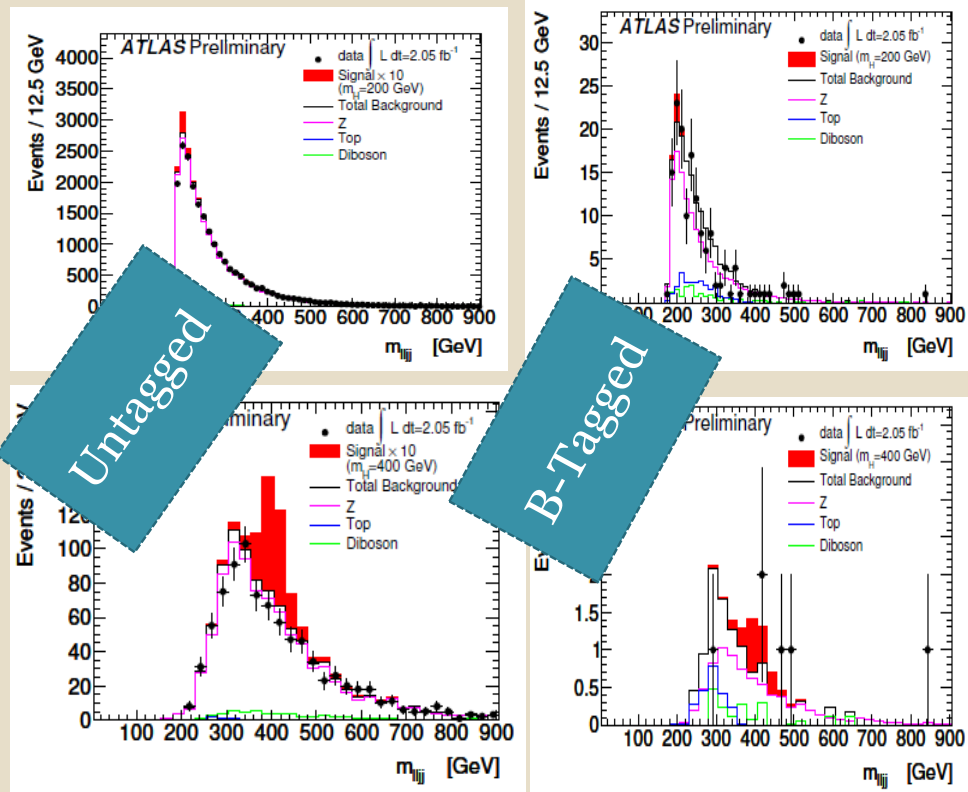
Top control
region



$H \rightarrow ZZ \rightarrow l^+l^-q\bar{q}$ ($l=e$ or μ): Results

39

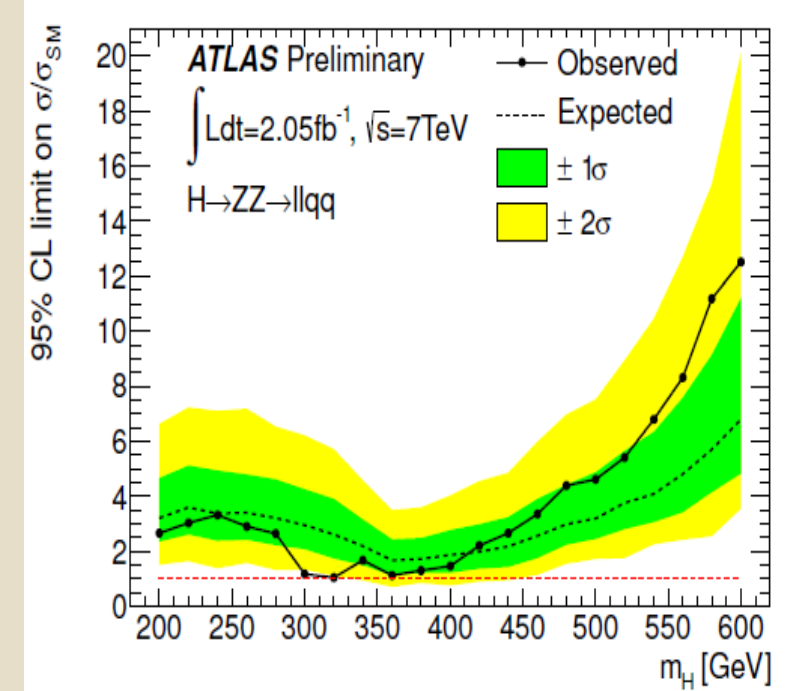
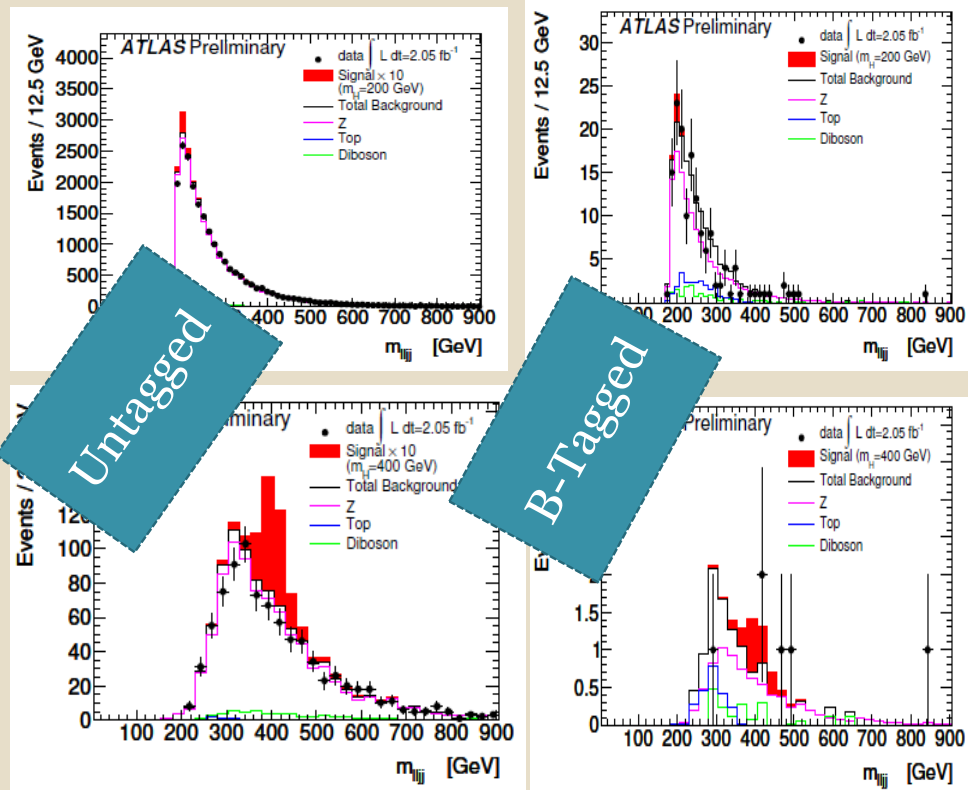
Final discriminant $M(ljj)$



$H \rightarrow ZZ \rightarrow l^+l^-q\bar{q}$ ($l=e$ or μ): Results

40

Final discriminant $M(ljj)$



No SM exclusion yet

$H \rightarrow ZZ \rightarrow l^+l^- \nu\bar{\nu}$ ($l = e$ or μ): Selection

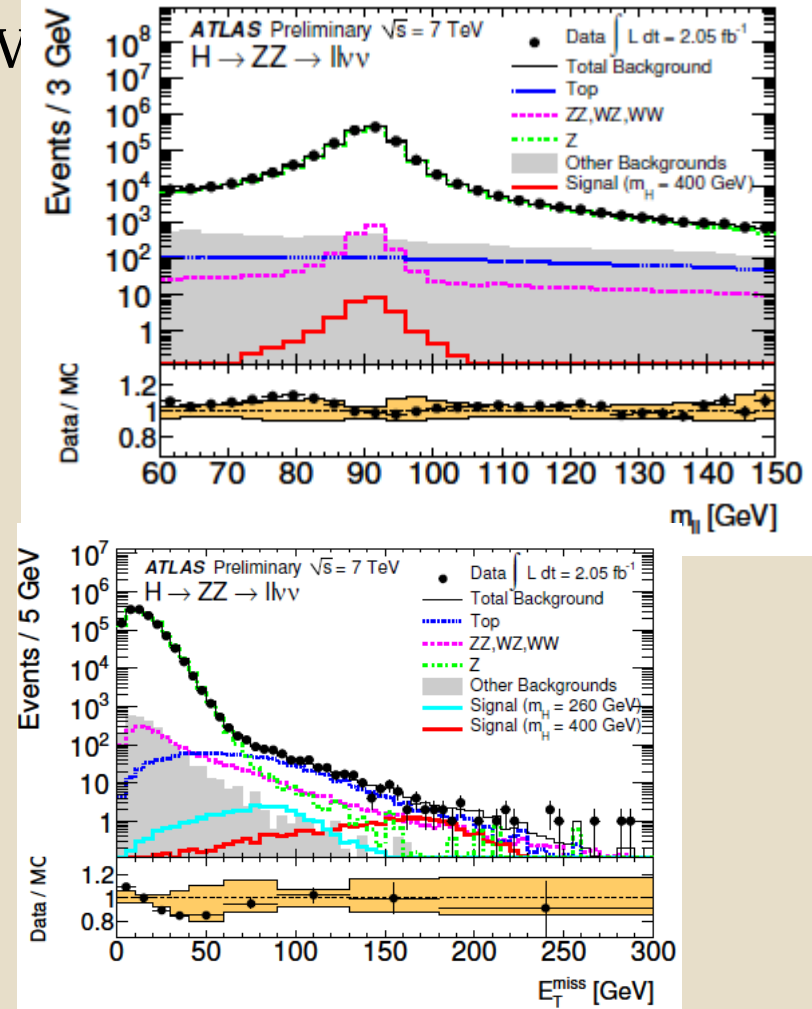
41

- Require isolated leptons with $P_T > 20\text{GeV}$
- $M_{ll} \in [M_Z \pm 15]$
- ETmiss
- If jets require to be far from ETmiss

$H \rightarrow ZZ \rightarrow l^+l^-v\bar{v}$ ($l = e$ or μ): Selection

42

- Require isolated leptons with $P_T > 20\text{ GeV}$
- $M_{ll} \in [M_Z \pm 15]$
- E_T^{miss}
- If jets require to be far from E_T^{miss}



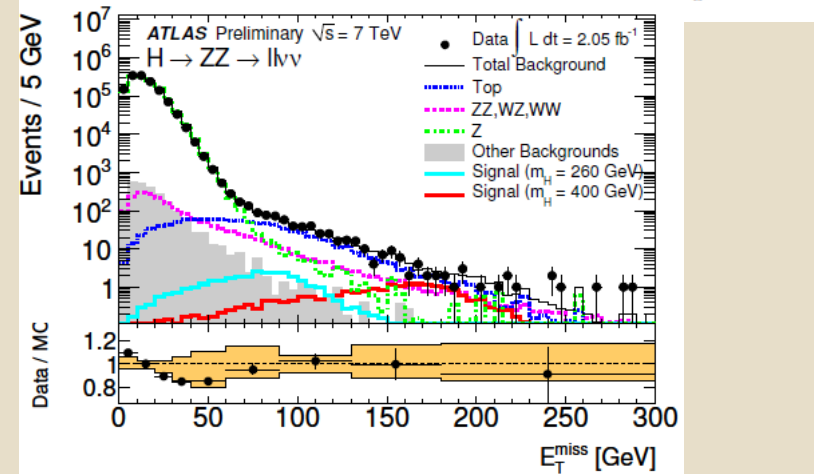
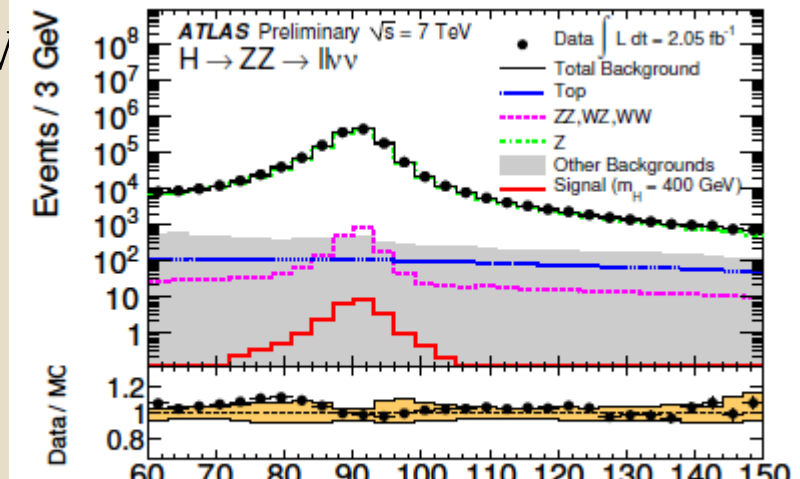
$H \rightarrow ZZ \rightarrow l^+l^-v\bar{v}$ ($l = e$ or μ): Selection

43

- Require isolated leptons with $P_T > 20\text{ GeV}$
- $M_{ll} \in [M_Z \pm 15]$
- E_T^{miss}
- If jets require to be far from E_T^{miss}

Backgrounds

- Main reducible: $Z + \text{jets}$ and $t\bar{t}$ from data driven methods
- ZZ , WW from MC



H \rightarrow ZZ \rightarrow l⁺l⁻ $\nu\bar{\nu}$ (l=e or μ): Backgrounds

44

→ High M_H hypothesis (>280GeV):

E_{Tmiss}>82GeV

$\Delta\Phi(l\bar{l}) < 2.25$

$\Delta\Phi(E_{Tmiss}, P_T(l\bar{l})) > 1$

→ Low M_H hypothesis (<280GeV):

E_{Tmiss}>66GeV and

$1 < \Delta\Phi(l\bar{l}) < 2.64$

H \rightarrow ZZ \rightarrow l⁺l⁻ $\nu\bar{\nu}$ (l=e or μ): Backgrounds

45

Discriminant variable :

$$m_T^2 \equiv \left[\sqrt{m_Z^2 + |\vec{p}_T^{\ell\ell}|^2} + \sqrt{m_Z^2 + |\vec{p}_T^{\text{miss}}|^2} \right]^2 - \left[\vec{p}_T^{\ell\ell} + \vec{p}_T^{\text{miss}} \right]^2$$

→ High M_H hypothesis (>280GeV):

Etmiss>82GeV

$\Delta\Phi(l\bar{l}) < 2.25$

$\Delta\Phi(\text{Etmiss}, P_T(l\bar{l})) > 1$

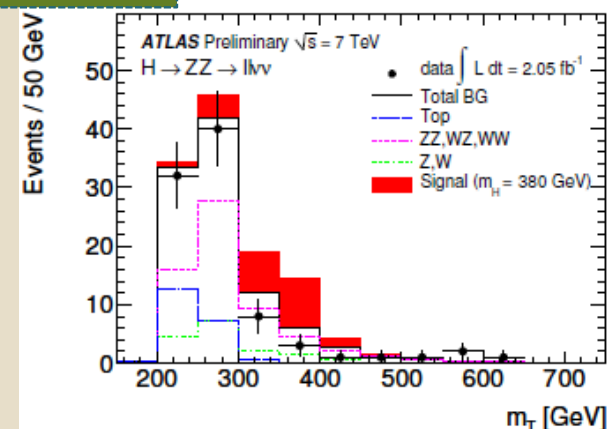
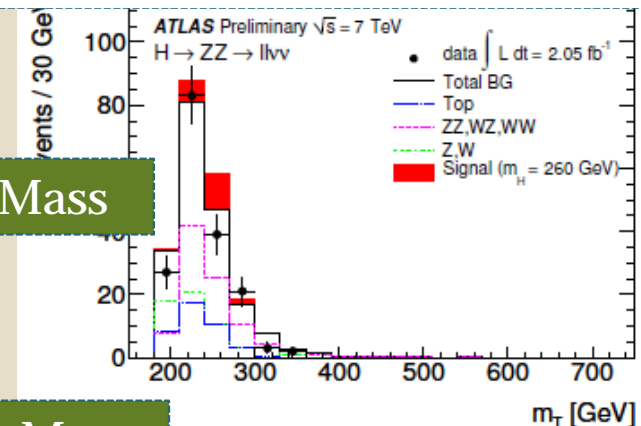
→ Low M_H hypothesis (<280GeV):

Etmiss>66GeV and

$1 < \Delta\Phi(l\bar{l}) < 2.64$

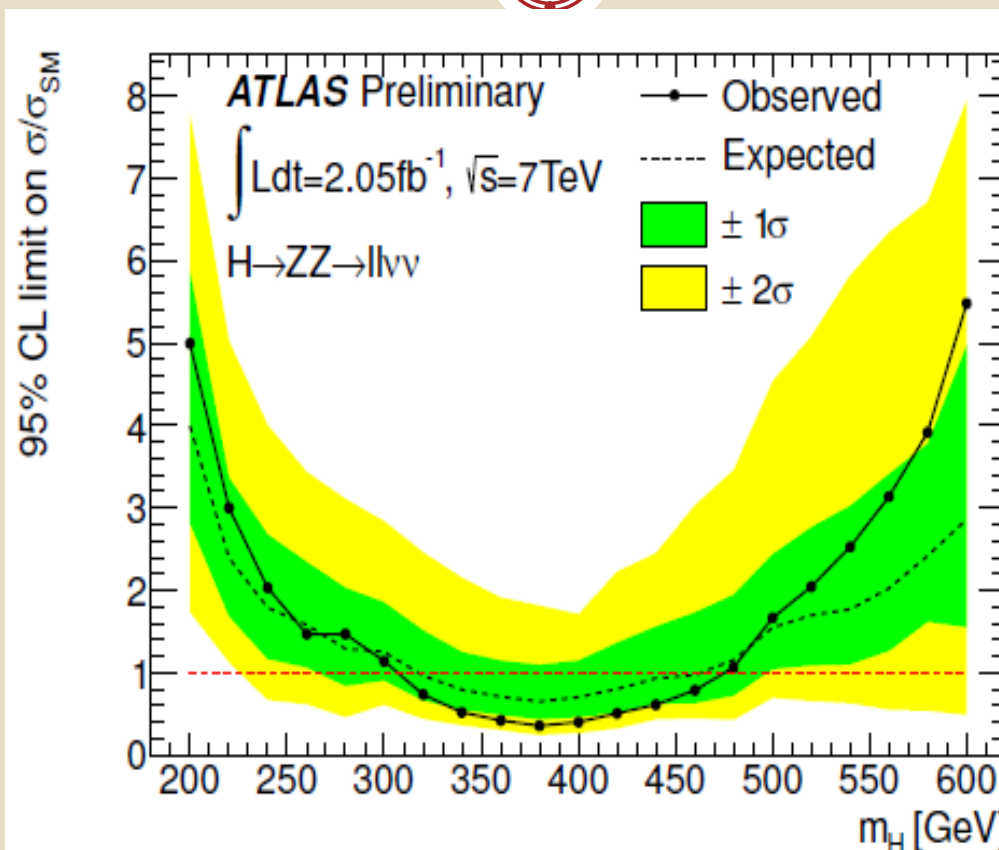
Low Mass

High Mass



$H \rightarrow ZZ \rightarrow l^+l^-v\bar{v}$ ($l=e$ or μ): Results

46



Exclusion:
310 - 470 GeV at 95%CL

$H \rightarrow ZZ^* \rightarrow 4l$ ($l=e$ or μ): selection

47

- The “GOLDEN” channel
- Allows M_H reconstruction with $fwhm \sim 5(35)\text{GeV}$ at $M_H = 130(400)\text{GeV}$
- Allows to probe low M_H through Z^* (performances at low P_T crucial!).
- All leptons $P_T > 7\text{ GeV}$ well identified and isolated .
- Require one $M_{ll} \in [M_Z \pm 15\text{GeV}]$
- Constraints on impact parameter

H \rightarrow ZZ* \rightarrow 4l (l=e or μ): selection

48

→ The “GOLDEN” channel

→ Allows M_H reconstruction with
 $fwhm \sim 5(35)\text{GeV}$ at $M_H = 130(400)\text{GeV}$

→ Allows to probe low M_H through Z^*
(performances at low P_T crucial!).

→ All leptons $P_T > 7\text{ GeV}$ well identified
and isolated .

→ Require one $M_{ll} \in [M_Z \pm 15\text{GeV}]$

→ Constraints on impact parameter

Main background: irreducible ZZ. From
MC normalized to the luminosity.

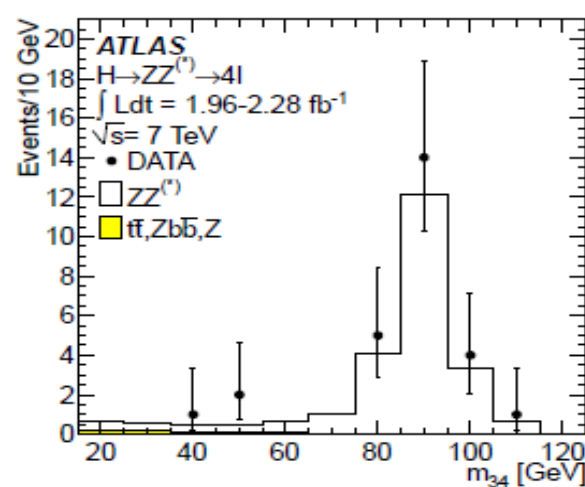
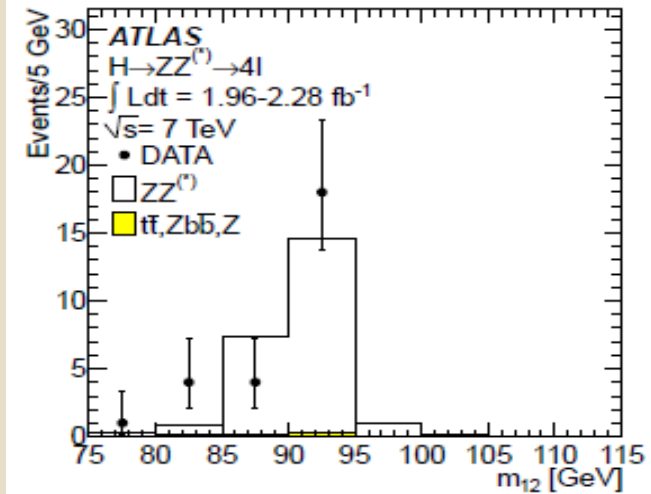
Other reducible: Z+light jets, $t\bar{t}$, Z+b \bar{b} ,
from data driven methods .

H \rightarrow ZZ* \rightarrow 4l (l=e or μ): selection

49

- The “GOLDEN” channel
- Allows M_H reconstruction with fwhm $\sim 5(35)$ GeV at $M_H=130(400)$ GeV
- Allows to probe low M_H through Z^* (performances at low P_T crucial!).
- All leptons $P_T > 7$ GeV well identified and isolated .
- Require one $M_{ll} \in [M_Z \pm 15]$ GeV
- Constraints on impact parameter

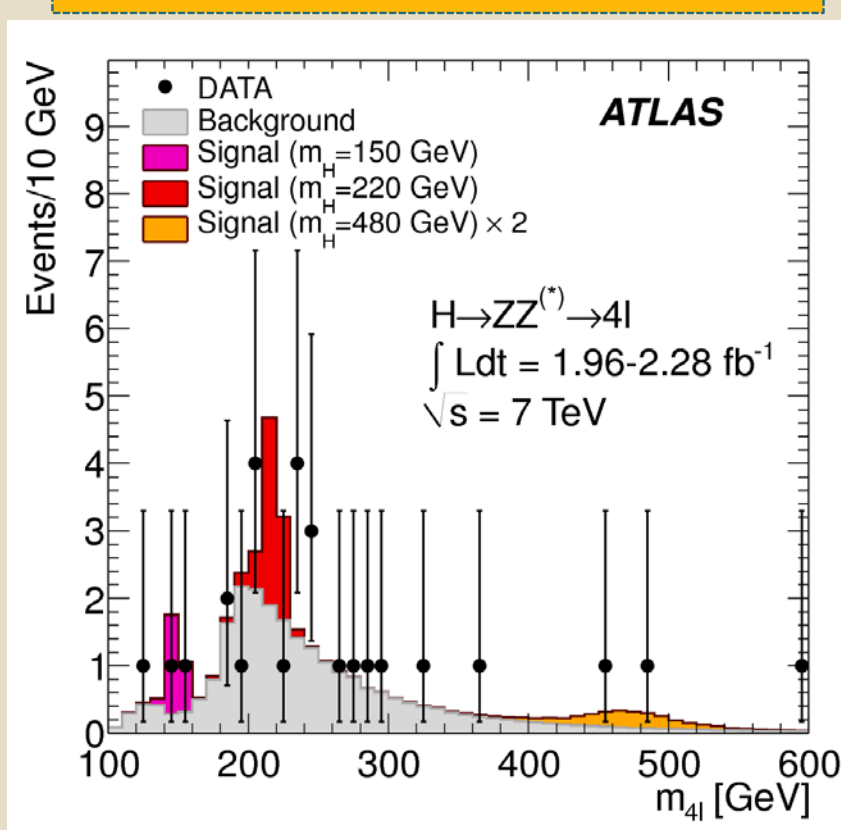
Main background: irreducible ZZ. From MC normalized to the luminosity.
Other reducible: Z+light jets, tt, Z+b \bar{b} , from data driven methods .



$H \rightarrow ZZ^* \rightarrow 4l$ ($l = e$ or μ): Results

50

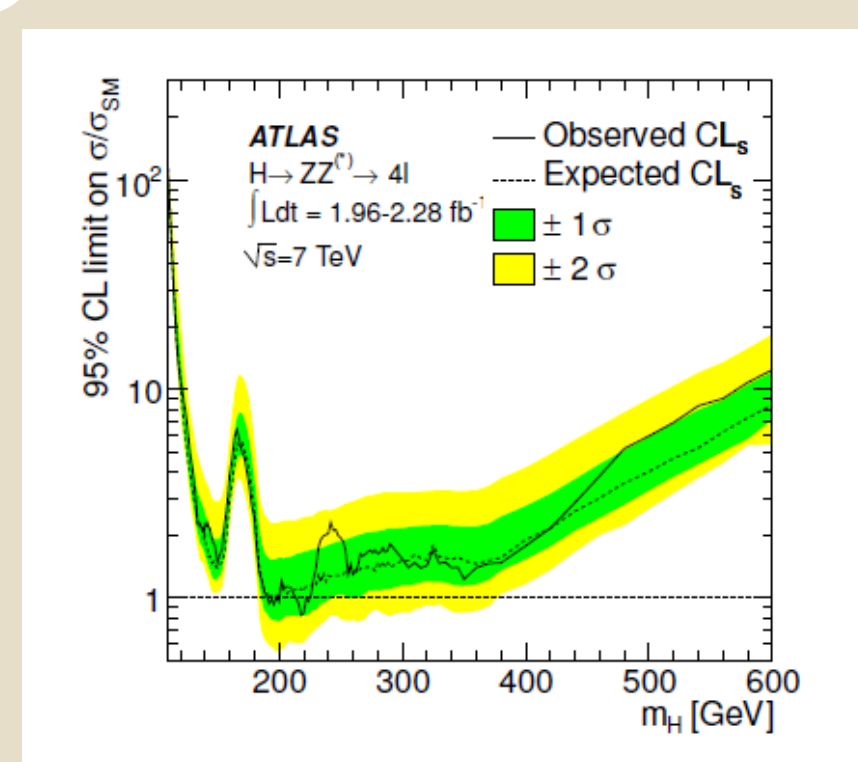
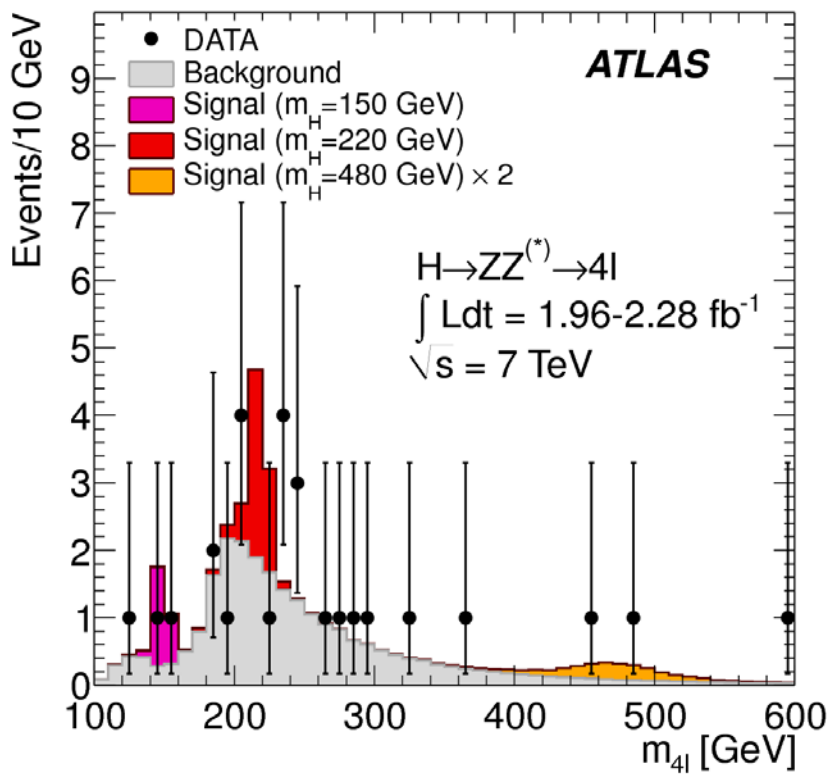
Final discriminant: $M(4l)$



H \rightarrow ZZ * \rightarrow 4l (l=e or μ): Results

51

Final discriminant: M (4l)



m_H (GeV) excluded in 95%CL :
 191-197, 199-200 and 214-224

Conclusions and Prospects

52

→ ATLAS collaboration has provided updated exclusion limits for SM Higgs decays in diboson channels. No excess has been observed.

Other results:

- Searches at low M_H : see talk by Michael Duehrssen-Debling
- Combined ATLAS result : see talk by Fabien Tarrade.

→ Next milestones:

- December: Higgs channels with full statistics.
- Winter conferences : Update with optimised object performances and analyses.

Conclusions and Prospects

53

→ ATLAS collaboration has provided updated exclusion limits for SM Higgs decays in diboson channels. No excess has been observed.

Other results:

- Searches at low M_H : see talk by Michael Duehrssen-Debling
- Combined ATLAS result : see talk by Fabien Tarrade.

→ Next milestones:

- December: Higgs channels with full statistics
- Winter conferences : Update with optimised object performances and analyses.

Thank you !



54

BACKUP

Systematics of $Z \rightarrow ll$ qq

55

Source of Uncertainty	Treatment in analysis
Jet Energy Scale (JES)	2 – 7% as a function of p_T and η
Jet Pile-up Uncertainty	3 – 7% as a function of p_T and η
b-quark Energy Scale	2.5%
Jet Energy Resolution	1-4%
Electron Selection Efficiency	0.7 – 3% as a function of p_T , 0.4 – 6% as a function of η
Electron Reconstruction Efficiency	0.7 – 1.8% as a function of η
Electron Energy Scale	0.1-6% as a function of η , pileup, material effects etc.
Electron Energy Resolution	Sampling term 20%, a small constant term has a large variation with η
Muon Selection Efficiency	0.2-3% as a function of p_T
Muon Trigger Efficiency	< 1%
Muon Momentum Scale	2-16% η dependent systematic on scale
Muon Momentum Resolution	p_T and η dependent resolution smearing functions, systematic $\leq 1\%$
b-tagging Efficiency	5-15% as a function of p_T
b-tagging Mis-tag Rate	10-22% as a function of p_T and η
Missing Transverse Energy	Propagate object uncertainties to E_T^{miss}

Number of events in $H \rightarrow ZZ \rightarrow llqq$ (2.05fb^{-1})

56

	Untagged			Tagged		
	Low- m_H	High- m_H	Low- m_H	High- m_H		
Z+jets	$20672 \pm 110 \pm 310$	$858 \pm 20 \pm 61$	126	$\pm 1 \pm 26$	$7.6 \pm 0.2 \pm 1.6$	
W+jets	$20 \pm 4 \pm 10$	$0.8 \pm 0.5 \pm 0.4$		< 0.1		< 0.1
Top	$85 \pm 2 \pm 11$	$6.4 \pm 0.5 \pm 1.1$	24	$\pm 1 \pm 5$	$2.2 \pm 0.4 \pm 0.5$	
Multijet	$87 \pm 3 \pm 87$	$2.1 \pm 0.5 \pm 2.1$		$0.1 \pm 0.1 \pm 0.1$		< 0.1
ZZ	$214 \pm 7 \pm 28$	$17.2 \pm 1.8 \pm 2.8$		$14.0 \pm 1.5 \pm 3.8$	$1.7 \pm 0.5 \pm 0.5$	
WZ	$292 \pm 6 \pm 56$	$34 \pm 2 \pm 6$		$0.6 \pm 0.3 \pm 0.3$		< 0.1
Total background	$21369 \pm 110 \pm 332$	$919 \pm 20 \pm 62$	165	$\pm 2 \pm 27$	$11.6 \pm 0.6 \pm 1.8$	
Data	21032	851		145		6
Signal						
$m_H = 200 \text{ GeV}$	$64 \pm 1 \pm 12$			$4.4 \pm 0.4 \pm 1.1$		
$m_H = 300 \text{ GeV}$		$14.0 \pm 0.5 \pm 2.9$			$1.2 \pm 0.1 \pm 0.3$	
$m_H = 400 \text{ GeV}$		$21.1 \pm 0.5 \pm 3.8$			$2.1 \pm 0.2 \pm 0.6$	
$m_H = 500 \text{ GeV}$		$11.5 \pm 0.2 \pm 2.1$			$1.3 \pm 0.1 \pm 0.4$	
$m_H = 600 \text{ GeV}$		$5.4 \pm 0.1 \pm 1.0$			$0.5 \pm 0.0 \pm 0.2$	

Event yields for H \rightarrow ZZ \rightarrow llvv (2.05fb $^{-1}$)

57

Source	low m_H search	high m_H search
Z + jets	$40.5 \pm 4.1 \pm 3.1$	$9.9 \pm 2.1 \pm 3.6$
W + jets	$17 \pm 4 \pm 17$	$6.1 \pm 1.7 \pm 6.1$
top	$40 \pm 1 \pm 12$	$20.9 \pm 1.0 \pm 6.2$
Multijet	$1.2 \pm 0.7 \pm 0.6$	$0.4 \pm 0.4 \pm 0.2$
ZZ	$35.1 \pm 0.7 \pm 4.1$	$29.6 \pm 0.6 \pm 3.5$
WZ	$32.4 \pm 1.0 \pm 3.8$	$23.2 \pm 0.8 \pm 2.7$
WW	$25.4 \pm 0.7 \pm 3.1$	$9.4 \pm 0.4 \pm 1.1$
Total BG	$192 \pm 6 \pm 35$	$100 \pm 3 \pm 17$
Data	175	89
m_H [GeV]	Signal expectation	s/b
200	$9.9 \pm 0.2 \pm 1.8$	8%
300	$19.9 \pm 0.3 \pm 3.5$	24%
400	$19.6 \pm 0.3 \pm 3.4$	57%
500	$8.8 \pm 0.1 \pm 1.5$	60%
600	$3.6 \pm 0.0 \pm 0.6$	60%

Experimental systematics in $H \rightarrow WW^* \rightarrow llvv$

Table 2: Experimental sources of systematic uncertainty per object or event.

Source of Uncertainty	Treatment in the analysis
Jet Energy Resolution (JER)	$\sim 14\%$, see Ref. [69]
Jet Energy Scale (JES)	Takes into account close-by jets effect, jet flavor composition uncertainty and event pile-up uncertainty in addition to global JES uncertainty Global JES $< 10\%$ for $p_T > 15$ GeV and $ \eta < 4.5$, see Ref. [70] Pile-up uncertainty 2-5% for $ \eta < 2.1$ and 3-7% for $2.1 < \eta < 4.5$ These are summed in quadrature before application.
Electron Selection Efficiency	Separate systematics for electron identification, reconstruction and isolation, added in quadrature Total uncertainty of 2-5% depending on η and E_T Uncertainty smaller than 1%, depending on η and E_T
Electron Energy Scale	Energy varied within its uncertainty, 0.6% of the energy at most
Electron Energy Resolution	0.3-1% as a function of η and p_T
Muon Selection Efficiency	η dependent scale offset in p_T , up to $\sim 0.13\%$
Muon Momentum Scale	p_T and η dependent resolution smearing functions, $\leq 5\%$
Muon Momentum Resolution	p_T dependent scale factor uncertainties, 5.6-15%, see Ref. [68]
b-tagging Efficiency	up to 21% as a function of p_T , see Ref. [68]
b-tagging Mis-tag Rate	13.2% uncertainty on topological cluster energy
Missing Transverse Energy	Electron and muon p_T changes from smearing propagated to MET Effect of out-of-time pileup: MET smeared by 5 GeV in 1/3 of MC events
Luminosity	3.7% [25]

Number of events of H+0 jet \rightarrow WW* \rightarrow l ν l ν (1.7fb $^{-1}$)

59

	Signal	WW	W + jets	Z/ γ^* + jets	$t\bar{t}$	tW/tb/tqb	WZ/ZZ/W γ	Total Bkg.	Observed
Jet Veto	82 ± 17	430 ± 40	70 ± 40	160 ± 150	37 ± 13	28 ± 7	11 ± 3	740 ± 160	738
$ \mathbf{P}_T^{\ell\ell} > 30 \text{ GeV}$	79 ± 17	390 ± 40	60 ± 30	28 ± 11	35 ± 12	25 ± 7	10 ± 3	540 ± 80	574
$m_{\ell\ell} < 50 \text{ GeV}$	56 ± 12	98 ± 13	17 ± 7	12 ± 7	6 ± 3	4.8 ± 1.5	1.2 ± 0.4	139 ± 20	175
$\Delta\phi_{\ell\ell} < 1.3$	48 ± 11	76 ± 10	9 ± 4	8 ± 6	5 ± 2	4.8 ± 1.5	1.1 ± 0.3	105 ± 16	131
$0.75 m_H < m_T < m_H$	34 ± 7	43 ± 6	5 ± 2	2 ± 4	2.2 ± 1.4	1.2 ± 0.8	0.7 ± 0.3	53 ± 9	70
ee	5.2 ± 1.2	6.2 ± 0.9	0.9 ± 0.4	0.8 ± 1.4	0.3 ± 0.3	0 ± 0.3	0.07 ± 0.05	8.2 ± 1.7	9
$e\mu$	17 ± 4	22 ± 3	2.8 ± 1.3	0 ± 1.3	1.1 ± 0.5	0.8 ± 0.6	0.31 ± 0.19	27 ± 4	32
$\mu\mu$	11 ± 2	14 ± 2	1.0 ± 0.6	1 ± 3	0.8 ± 1.1	0.4 ± 0.4	0.31 ± 0.09	18 ± 5	29

Event yields for H \rightarrow ZZ* \rightarrow 4l (2.1fb $^{-1}$)

60

	$\mu\mu\mu\mu$		$ee\mu\mu$		$eeee$	
	Low mass	High mass	Low mass	High mass	Low mass	High mass
Integrated Luminosity	2.28 fb $^{-1}$		1.96 fb $^{-1}$		1.98 fb $^{-1}$	
$ZZ^{(*)}$	1.02 \pm 0.15	7.7 \pm 1.2	0.99 \pm 0.16	9.6 \pm 1.4	0.39 \pm 0.09	3.6 \pm 0.5
$Z, Zb\bar{b}, t\bar{t}$	0.06 \pm 0.01	0.01 \pm 0.01	0.29 \pm 0.11	0.15 \pm 0.06	0.23 \pm 0.09	0.12 \pm 0.05
Total Background	1.08 \pm 0.15	7.7 \pm 1.2	1.28 \pm 0.19	9.8 \pm 1.4	0.62 \pm 0.13	3.7 \pm 0.5
Data	1	11	1	8	1	5
$m_H = 130$ GeV	0.42 \pm 0.07		0.40 \pm 0.06		0.14 \pm 0.03	
$m_H = 150$ GeV	0.98 \pm 0.15		0.97 \pm 0.15		0.34 \pm 0.06	
$m_H = 200$ GeV	2.26 \pm 0.33		2.64 \pm 0.38		0.98 \pm 0.14	
$m_H = 240$ GeV	1.74 \pm 0.25		2.24 \pm 0.32		0.88 \pm 0.13	
$m_H = 300$ GeV	1.18 \pm 0.17		1.64 \pm 0.23		0.64 \pm 0.09	
$m_H = 400$ GeV	0.86 \pm 0.13		1.23 \pm 0.18		0.52 \pm 0.08	
$m_H = 600$ GeV	0.15 \pm 0.02		0.23 \pm 0.04		0.10 \pm 0.02	

H \rightarrow WW* \rightarrow l ν jj

61

	H(evjj) + 0j	H($\mu\nu jj$) + 0j	H(evjj) + 1j	H($\mu\nu jj$) + 1j	H + 0j or 1j
W/Z+jets	10780 ± 290	13380 ± 870	6510 ± 250	7410 ± 670	38080 ± 1160
Multi-jet	890 ± 24	256 ± 17	669 ± 25	212 ± 19	2027 ± 43
Top	170 ± 34	164 ± 33	489 ± 98	500 ± 100	1320 ± 270
Dibosons	397 ± 79	414 ± 83	161 ± 32	204 ± 41	1180 ± 240
Expected Background	12240 ± 300	14210 ± 870	7830 ± 270	8330 ± 680	42600 ± 1200
Data	11988	13906	7543	8250	41687
Expected Signal ($m_H = 400$ GeV)	14 ± 3.6	12 ± 3.1	18 ± 4.7	14 ± 3.6	58 ± 15

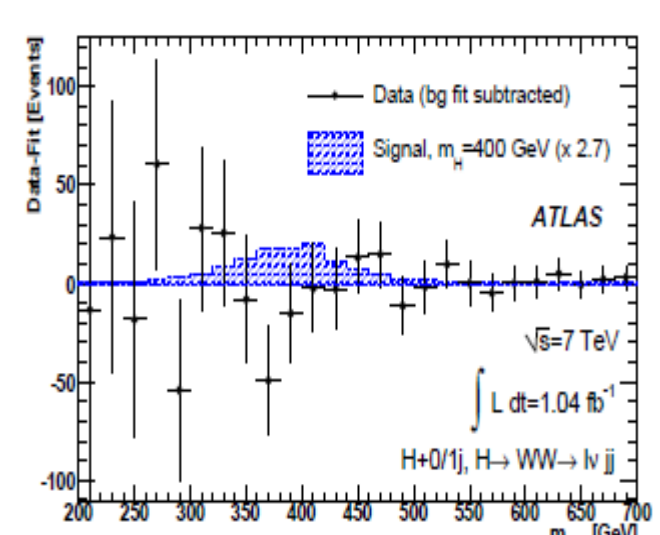


TABLE II: Expected and observed numbers of events for an integrated luminosity of 1.04 fb^{-1} after all selection cuts (except for the requirement that $m(l\nu) = m(W)$ has a real solution) for the signal and the main backgrounds. For the W/Z+jets and MJ backgrounds, the uncertainties are taken from the fit to the E_T distribution used to normalize these backgrounds.

